Journal of Biomedical Optics

BiomedicalOptics.SPIEDigitalLibrary.org

Review of clinical approaches in fluorescence lifetime imaging ophthalmoscopy

Lydia Sauer
Karl M. Andersen
Chantal Dysli
Martin S. Zinkernagel
Paul S. Bernstein
Martin Hammer

SPIE.

Lydia Sauer, Karl M. Andersen, Chantal Dysli, Martin S. Zinkernagel, Paul S. Bernstein, Martin Hammer, "Review of clinical approaches in fluorescence lifetime imaging ophthalmoscopy," *J. Biomed. Opt.* **23**(9), 091415 (2018), doi: 10.1117/1.JBO.23.9.091415.

Journal of Biomedical Optics 23(9), 091415 (September 2018)

REVIEW

Review of clinical approaches in fluorescence lifetime imaging ophthalmoscopy

Lydia Sauer,[a,b] Karl M. Andersen,[b,c] Chantal Dysli,[d] Martin S. Zinkernagel,[d] Paul S. Bernstein,[b] and Martin Hammer[a,e,*]

[a]University Hospital Jena, Jena, Thuringia, Germany
[b]University of Utah, John A. Moran Eye Center, Salt Lake City, Utah, United States
[c]Geisinger Commonwealth School of Medicine, Scranton, Pennsylvania, United States
[d]Bern University Hospital, Inselspital, Department of Ophthalmology, Bern, Switzerland
[e]University of Jena, Center for Biomedical Optics and Photonics, Jena, Germany

Abstract. Autofluorescence-based imaging techniques have become very important in the ophthalmological field. Being noninvasive and very sensitive, they are broadly used in clinical routines. Conventional autofluorescence intensity imaging is largely influenced by the strong fluorescence of lipofuscin, a fluorophore that can be found at the level of the retinal pigment epithelium. However, different endogenous retinal fluorophores can be altered in various diseases. Fluorescence lifetime imaging ophthalmoscopy (FLIO) is an imaging modality to investigate the autofluorescence of the human fundus *in vivo*. It expands the level of information, as an addition to investigating the fluorescence intensity, and autofluorescence lifetimes are captured. The Heidelberg Engineering Spectralis-based fluorescence lifetime imaging ophthalmoscope is used to investigate a 30-deg retinal field centered at the fovea. It detects FAF decays in short [498 to 560 nm, short spectral channel (SSC) and long (560 to 720 nm, long spectral channel (LSC)] spectral channels, the mean fluorescence lifetimes (τ_m) are calculated using bi- or triexponential approaches. These are meant to be relatively independent of the fluorophore's intensity; therefore, fluorophores with less intense fluorescence can be detected. As an example, FLIO detects the fluorescence of macular pigment, retinal carotenoids that help protect the human fundus from light damages. Furthermore, FLIO is able to detect changes related to various retinal diseases, such as age-related macular degeneration, albinism, Alzheimer's disease, diabetic retinopathy, macular telangiectasia type 2, retinitis pigmentosa, and Stargardt disease. Some of these changes can already be found in healthy eyes and may indicate a risk to developing such diseases. Other changes in already affected eyes seem to indicate disease progression. This review article focuses on providing detailed information on the clinical findings of FLIO. This technique detects not only structural changes at very early stages but also metabolic and disease-related alterations. Therefore, it is a very promising tool that might soon be used for early diagnostics.
 [DOI: 10.1117/1.JBO.23.9.091415]

Keywords: time-resolved fundus autofluorescence; fluorescence lifetime; retinal disease; lipofuscin; macular pigment; protein glycation; fluorescence lifetime imaging ophthalmoscopy.

Paper 180049SSVRR received Jan. 28, 2018; accepted for publication Jul. 24, 2018; published online Sep. 4, 2018; corrected Sep. 7, 2018.

1 Introduction

Fluorescence lifetime imaging ophthalmoscopy (FLIO) is an imaging modality that can be used to investigate the human fundus *in vivo*. In contrast to commonly used autofluorescence-based imaging modalities, the information obtained with FLIO is not based only on the intensity of individual fluorophores. As the main outcome measure, autofluorescence lifetimes (also called autofluorescence decay times) are investigated; these are independent of the fluorescence intensity and may be correlated to changes in the molecular composition of the human retina. Although the technique is relatively new, many diseases have already been investigated. Researchers have discovered very specific disease-related changes, which could be helpful in the early diagnosis as well as the follow-up of different diseases. This review article aims to give an overview of the clinical applications of FLIO. This may be helpful to establish the use of FLIO in the clinical routine. After briefly explaining the methodology of the FLIO technique, different clinical applications will be emphasized. This review includes a detailed description of FLIO findings in the healthy eye, as well as age-related macular degeneration (AMD), diabetic retinopathy (DR), macular telangiectasia type 2 (MacTel), albinism, retinal vessel occlusion, Stargardt disease, central serous chorioretinopathy (CSCR), choroideremia, retinitis pigmentosa (RP), and Alzheimer's disease. Furthermore, mouse models will only briefly be discussed, as they may eventually help in understanding the contribution of single fundus layers to the sum fluorescence. They may help to interpret fluorescence changes in relationship to pathomechanisms behind different diseases. Finally, we will discuss the current state of FLIO research and try to give an outlook from our own perspective on possible future significances of the FLIO methodology.

2 Fluorescence Lifetime Imaging

2.1 *Basic Principles of Fluorescence*

Fluorescence is defined as the emission of radiation, especially visible light, by a substance during exposure to external

*Address all correspondence to: Martin Hammer, E-mail: martin.hammer@med.uni-jena.de

1083-3668/2018/$25.00 © 2018 SPIE

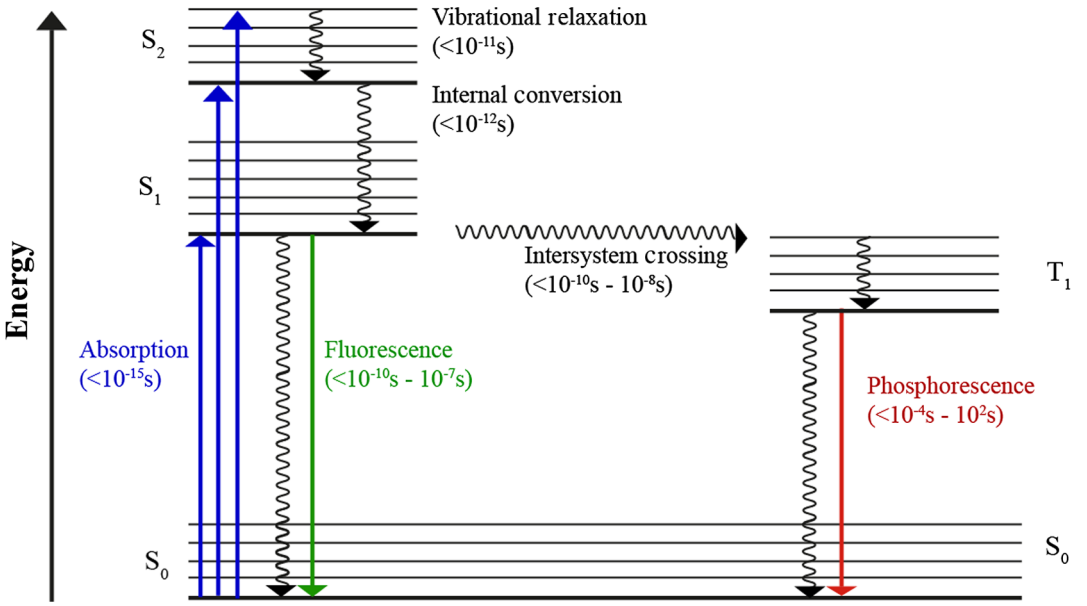

Fig. 1 The Perrin–Jablonski diagram highlights the photophysical processes involved in fluorescence and phosphorescence.

radiation. Alexander Jablonski developed the Perrin–Jablonski diagram to show the corresponding relations (Fig. 1).

The diagram shows different energy levels that may be occupied by electrons. Electrons possess an intrinsic angular momentum, characterized by the spin quantum number ($-1/2$ or $+1/2$). The electron energy of a system can show the values $S = 0$, $S = 1$, or higher. Here, $S = 0$ describes that the system is in the singlet state (S), the ground state; $S = 1$ denotes the first excited states with different vibratory and rotational conditions.[1]

When a photon of appropriate energy impacts a molecule, the energy is absorbed and an electron is transferred to a higher energetic level retaining the spin quantum number. Internal conversion describes radiationless crossings to the lowest vibrational state of the excited levels. After a certain time, electrons relax to the ground state, usually by emitting fluorescence photons with a wavelength of the energy difference between excited and ground states. Due to the transformation of energy during internal conversion, emitted photons have a longer wavelength as compared with the excitation radiation (Stokes-shift).

The fluorescence lifetime τ is defined as the mean time that a molecule remains in the excited state, before emitting a photon and falling back to the ground state. The fluorescence lifetime τ is an intrinsic and characteristic property of each fluorophore, based on the rate of photo-emitting (k_r) and radiationless (k_{nr}) crossings rates according to

$$\tau = \frac{1}{k_r + k_{nr}}. \tag{1}$$

The lifetime τ can be determined from the exponential decay of the fluorescence over time t

$$I(t) = I_0 * e^{-\frac{t}{\tau}}. \tag{2}$$

The intensity (I) is the emitted radiant power, showing proportionality to the amount of molecules in the excited state. I_0 describes the intensity at $t = 0$. In cases of monoexponential decays, τ equals the time that has passed until I has dropped to 1/e of the I_0-value.

In cases of organic tissue, such as the eye, a multiplicity of different fluorophores can be found, resulting in multiexponential decays. In these cases, the decay is a series of exponentials ($i = 1 \ldots n$, $n \in N$)

$$\frac{I(t)}{I_0} = \sum_i^n \alpha_i * e^{-\frac{t}{\tau_i}}. \tag{3}$$

The amplitudes α_i describe the relative fraction of each fluorescence component to the total fluorescence. The concentration of a fluorophore impacts α. Figure 2 shows the fluorescence decay of different fluorophores, as well as the summed fluorescence signal.

Using a triexponential approach, fluorescence decays, as found *in vivo* at the human eye, can be characterized. This is established to give the amplitude-weighted mean fluorescence lifetime τ_m to characterize the mean multiexponential decay characteristics. τ_m is calculated according to

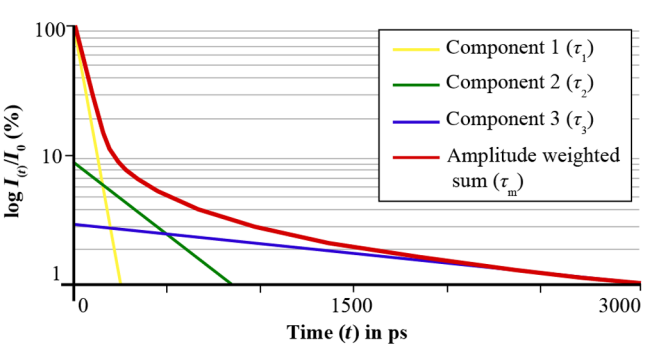

Fig. 2 The graph schematically shows the mechanism of a triexponential approximation to obtain the amplitude weighted mean autofluorescence lifetime τ_m. The fluorescence intensity (y-axis) is depicted over the time t (x-axis). τ_m is calculated based on the amplitudes and the sum of three exponential functions (components 1 to 3).

$$\tau_m = \frac{\sum_{i=1}^{n}(\tau_i * \alpha_i)}{\sum_{i=1}^{n}\alpha_i}. \quad (4)$$

Q_i describes the relative fraction of lifetime components (i) on the total fluorescence

$$Q_i = \frac{(\tau_i * \alpha_i)}{\sum_{i}^{n}(\tau_i * \alpha_i)}. \quad (5)$$

Fluorescence lifetime is considered to be independent of perturbation conditions such as duration of light exposure, intensity, concentration, and photobleaching.

In this paper, we review the application of fluorescence lifetime imaging in ophthalmology. We briefly address *in vitro* microscopy but focus on the clinical *in vivo* application.

2.2 *In Vitro Fluorescence Detection: Fluorescence Lifetime Imaging Microscopy*

Fluorescence-based microscopy techniques have become important tools for tissue imaging and open new possibilities for investigating the tissue behavior in response to different influences at a molecular level.[2] One of many fluorescence-based microscopic imaging modalities is the fluorescence lifetime imaging microscopy (FLIM), which has successfully been used to investigate biological processes in human tissue, as well as on the cellular level.[3] The principle of time-correlated single photon counting (TCSPC) is used for FLIM in this context.[4] As TCSPC-FLIM relies on short pulse laser illumination, it can easily be combined with two-photon excitation, which allows three-dimensional imaging of bulk tissue.

Recently, FLIM techniques based on two-photon excitation were used in imaging of ocular tissue.[5–9] Due to the high resolution and possibility of molecular imaging, it has become a promising tool in ophthalmological research, for example, in studies related to AMD.[6,8] In two-photon excitation imaging modalities, two photons of long wavelength are simultaneously absorbed, inducing the transfer of a molecule to an excited state. Based on this concept, which was predicted by Maria Goeppert-Mayer in 1931 and later verified by Kaiser and Garrett, two-photon excitation was later combined with scanning laser microscopy, which provides the foundation of FLIM.[10–12] Due to the long wavelength excitation, used in this technique, light scattering of tissue is reduced.[13,14] Fluorescence lifetimes of ocular tissues have been investigated and described previously. Peters et al.[9] used two-photon FLIM to measure fluorescence lifetimes in porcine retina and retinal pigment epithelium (RPE), which were found to be very short (<100 ps) in the RPE due to melanin fluorescence and on the order of several 100 ps in the retina. Fluorescence lifetimes might be influenced by their environment and other factors, such as the pH-value and the oxidation level.[9,15–19] For example, different redox states of nicotinamide adenine dinucleotide (NADH) and flavin adenine dinucleotide (FAD) were successfully monitored.[20,21] However, the use of this technique in ophthalmology is still under investigation.[6,8,12,22–25] Recently, the redox state of Müller cells under oxidative stress, as well as hypoxia and the protein binding of NAD(P)H in their mitochondria, were investigated.[26,27] A comparison of results from FLIM studies with *in vivo* imaging might be helpful in taking this technique to a new level. This is now possible, as Schweitzer et al.[28] developed an FLIM-based scanning laser ophthalmoscope for *in vivo* ocular imaging of autofluorescence lifetimes.

2.3 *In Vivo Fluorescence Detection: Fluorescence Lifetime Imaging Ophthalmoscopy*

The autofluorescence of the retina was first discovered in early days of fluorescein angiography imaging when fluorescence was detected even before a fluorescent dye was injected.[29,30] Such fluorescence is based on the accumulation of hyperfluorescent material, such as the age-related pigment lipofuscin within the RPE. Now, imaging fundus autofluorescence (FAF) intensity is a noninvasive and standardized application in clinical routines to investigate the metabolic state of the retina. An important fluorophore is *N*-retinylidene-*N*-retinylethanolamine (A2E), which is present in lipofuscin granules within the RPE.[18,31] With FAF imaging, information about the spatial distribution of fluorescence intensity is captured. Changes within the chemical composition cannot be detected, and a specific assignment to chemical compounds cannot be made.[32,33] Furthermore, lipofuscin emits fluorescence in high intensity and therefore overwhelms the fluorescence of other compounds.[18,34]

In fluorescence lifetime imaging, the signal depends on inherent properties of each fluorophore. Each fluorophore has a characteristic autofluorescence lifetime.[35] Investigating the FAF lifetime has the advantage that molecules with overlapping fluorescence emission spectra but different autofluorescence lifetimes can be distinguished; thus, even small microenvironmental changes may be detected. Furthermore, FAF lifetimes are mostly independent of the fluorescence intensity.[35–37]

Schweitzer et al.[28] combined time-resolved fluorescence imaging with scanning laser ophthalmoscopy and revealed a setup for *in vivo* imaging. The technique was later combined with the Heidelberg Engineering (Heidelberg, Germany) Spectralis® System and is known as FLIO. Similar to FLIM, FLIO also relies on the principle of TCSPC.[4] In contrast to monoexponential probes with only one fluorophore, the human retina holds different fluorophores, resulting in multiexponential autofluorescence decays at the fundus. Changes in these autofluorescence lifetimes may lead to specific information about the configuration of fluorescent molecules and their embedded environmental matrix.[15,38,39] FLIO has been used to investigate healthy eyes, as well as several retinal diseases.[16,40–51]

2.4 *FLIO Setup*

FLIO combines TCSPC with confocal scanning laser ophthalmoscopy. Figure 3 shows the basic setup of this device. It excites the retinal fluorescence with a 473-nm pulsed diode laser, emitting with 89-ps full width at half maximum pulses at 80-MHz repetition frequency. FLIO conforms to international safety standards, such as the International Electrotechnical Commission (IEC 60825-1:2007) standard and the American National Standards Institute (ANSI Z136.1-2000) standard. The laser power used in FLIO is well below the hereby required maximum allowances for both standards. Detailed calculations on the safety have been published.[45]

FLIO investigates a 30 deg × 30 deg retinal field, which has usually been centered at the fovea. This refers to an area with the size of 9×9 mm^2 at the retina. Each FLIO image consists of 256×256 pixels which results in a spatial resolution of 35 μm in emmetropic eyes. The FLIO imaging field can be moved to various spots at the retina, such as the optic disc. However,

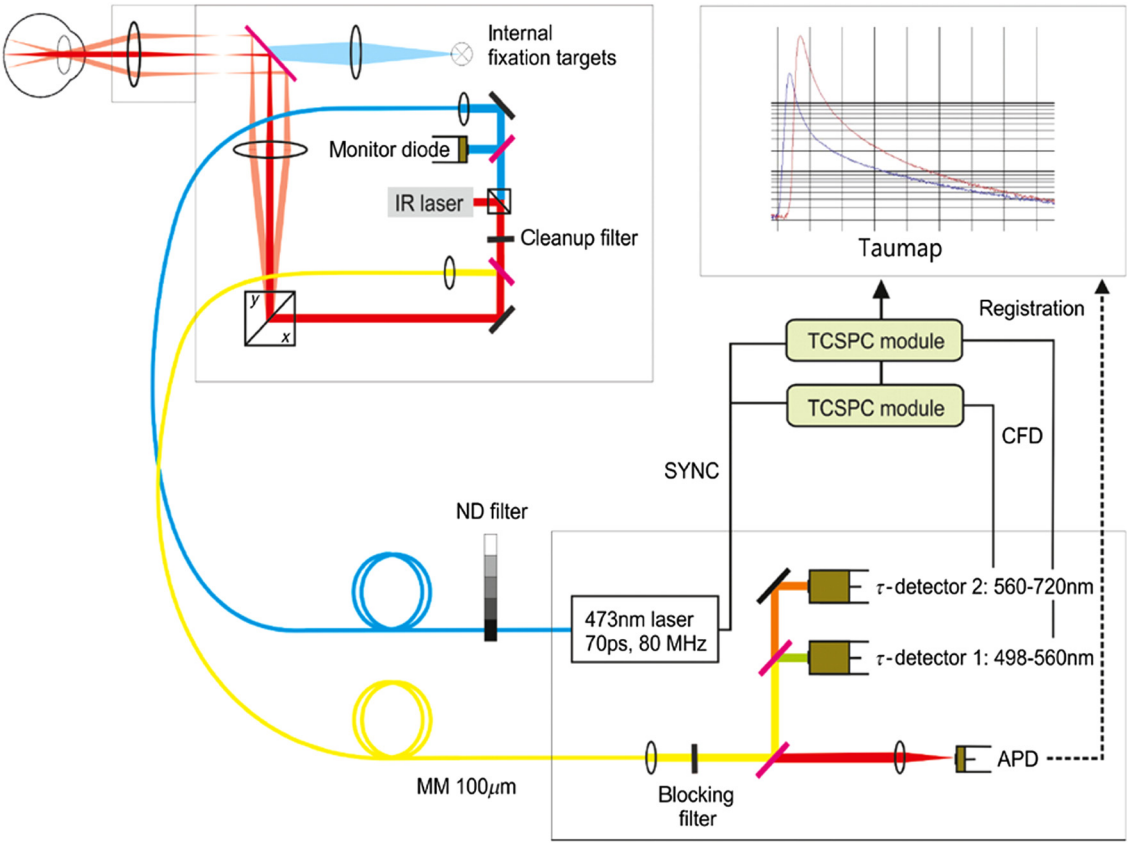

Fig. 3 The basic setup of the scanning fluorescence lifetime imaging ophthalmoscope is depicted. A pulsed 473-nm laser excites retinal fluorescence in a 30-deg field. Fluorescence photons are then detected according to their wavelength in two spectral channels (1: short spectral channel, SSC: 498 to 560 nm; 2: long spectral channel, LSC: 560 to 720 nm). An infrared (IR) laser is used for eye tracking.

so far only foveal-centered images have been thoroughly investigated. The fluorescence photons, emitted from retinal tissue after short laser pulse excitation, are recorded individually in a time-resolved manner. For compensation of eye movements, a high-contrast confocal infrared reflectance (IR) image for eye tracking is utilized. With this technique, each fluorescence photon is recorded in the dedicated time channel and analyzed at its correct spatial position. Two hybrid photon-counting detectors (HPM-100-40; Becker & Hickl GmbH, Berlin, Germany) count the emitted photons in two separate spectral channels, a short wavelength channel (498 to 560 nm, SSC) and a long wavelength channel (560 to 720 nm, LSC). These channels were chosen based on previous studies.[15]

For each pixel, the photon counting into one of 1024 time channels results in a photon arrival histogram, which represents the fluorescence decay with a resolution of 12.2 ps. As minimum signal threshold, at least 1000 photons are recorded in each pixel, taking an acquisition time of ~2 min.

Different software can be used to approximate the autofluorescence decay, such as FLIMX or SPCImage (Becker & Hickl GmbH), the latter being the most commonly used software in FLIO investigations.[52,53] The photon arrival decay in each of the 65,536 pixels is hereby approximated according to

$$\frac{I(t)}{I_0} = \mathrm{IRF} \otimes \sum_i a_i * e^{\frac{-t}{\tau i}}. \quad (6)$$

This is based on Eq. (3); $\otimes$ indicates the convolution integral with the instrument response function (IRF). Bi- and triexponential decays were previously used to investigate the retinal fluorescence *in vivo*. A triexponential approach leads to three different lifetimes ($\tau 1, \tau 2$, and $\tau 3$) as well as their three amplitudes, which represent their proportion of the total fluorescence lifetime.

As the FAF *in vivo* typically does not completely decay within 12.5 ns (time between two excitation pulses upon 80-MHz laser repetition rate), the application of an incomplete multiexponential decay mode is standard. Although the theoretical time resolution should be 12.2 ps (1/80 MHz/1024 = 12.5 ns/1024 = 12.2 ps). As at least three supporting points are necessary for reconstruction of a decay, the shortest detectable lifetimes are about 30 ps.[45] For further data analysis, image processing, and especially to average FAF lifetimes over certain regions of interest, different software packages have been used. The FLIO-reader (ARTORG Center for Biomedical Engineering Research, University of Bern, Bern, Switzerland) and the software FLIMX (Institute of Biomedical Engineering and Informatics, Technische Universität Ilmenau, Ilmenau, Germany) are common.[52]

3 Fluorescence Lifetimes of Different Retinal Fluorophores

Within the human retina *in vivo*, many different fluorophores can be found. A previous review article about FLIO describes

a variety of retinal fluorophores in detail, with a focus on natural endogenous retinal fluorophores measured with FLIM.[16] In addition, a broad compilation of lifetimes of endogenous fluorophores from the literature was given by Schweitzer[54] previously. Therefore, we keep the presentation of these substances in this article short and focus on a compact description of the most important retinal fluorophores.

3.1 *Lipofuscin*

In the context of retinal fluorescence, lipofuscin is a well-known fluorophore. It is uniquely responsible for a large contribution to the retinal fluorescence and is very well characterized. As the dominant fluorophore at the posterior pole, it emits fluorescence with high intensity.[18] It appears in almost all phagocytes. Within the eye, it can be found in the RPE where it is developed through oxidative processes in the degradation of photoreceptor outer segments.[55] Lipofuscin accumulation is a general sign of cell aging; therefore, the amount of lipofuscin increases with increasing age.[56] Possibly also through this mechanism, FAF lifetimes at the human fundus increase with age.[40] Another reason for increased FAF lifetimes with age could also be the aging of the lens.[40] Lipofuscin was investigated by Eldred und Katz in 1988, and further studies were conducted to better understand the constituent parts of RPE granules.[57,58] Sparrow et al. were able to identify at least 25 different bisretinoids.[59] Lipofuscin, with an excitation maximum of around 340 to 395 nm, shows two emission maxima (430 to 460 nm and 540 to 640 nm).[60] The main component of the fluorescence is emitted by the hydrophobic A2E with a maximum at an excitation wavelength of 446 nm and an emission maximum at roughly 600 nm. It shows a mean autofluorescence lifetime of ~189 ps ($\tau_1 = 0.17$ ns, $\alpha_1 = 98\%$; $\tau_2 = 1.12$ ns, $\alpha_2 = 2\%$).[15] It is assumed that A2E may damage cell membranes by released radicals in a photochemical reaction, and the molecule has been reported to be related to the development of a variety of retinal diseases such as AMD.[61,62] However, the dominance of A2E on the development of retinal diseases has recently been discussed controversially, as it is possible that A2E isoforms or even other lipofuscin components could be involved in damaging the retina.[63] In addition, it was shown that there is no relation between A2E and an increasing FAF intensity with increasing age.[64] Therefore, phototoxic theories regarding A2E are still under discussion.[65]

3.2 *Retinal Carotenoids*

The macular pigment (MP) consists of the carotenoids lutein (L), zeaxanthin (Z), and meso-zeaxanthin (MZ).[66,67] These yellow-colored pigments can be found anterior to the photoreceptors, especially within the Müller-cells and the Henle fiber layer.[68,69] Xanthophyll-binding proteins can be found in a circular area of 0.5 mm in diameter centered at the fovea, resulting in an accumulation of MP this region.[70–76] The carotenoids protect the cells at the macula from oxidative damages by absorbing especially within the blue-light range (around 460 nm) and therefore act as protective antioxidants.[70,77,78] According to Bone et al.,[69,79–81] two protective mechanisms are possible: MP may quench free radicals and absorb the potentially phototoxic blue light before reaching the photoreceptor layer.

The absorption of the blue fluorescence excitation light by carotenoids in the fovea causes a hypofluorescent (dark) area in FAF intensity images in the macular center.[33] Therefore, it has been believed that *in vivo* MP does not show any fluorescence within the retina. However, one study using Raman-based imaging showed direct fluorescence from retinal carotenoids.[82,83] Later, FAF lifetime imaging was able to prove this fluorescence.[45] This was possible because FAF lifetimes are independent of the intensity of fluorescence, so carotenoids with weak fluorescence intensity also impact the measured autofluorescence lifetimes of the fundus.[45,84]

3.3 *Redox Equivalents*

Different redox equivalents, such as NADH, FAD, and flavin-mononucleotide (FMN), may impact FAF lifetimes, as their fluorescence properties may depend on the redox state of tissues.

NADH mostly shows fluorescence in the reduced form, and NAD+ (oxidized form) shows only a very weak fluorescence.[35,85,86] While free NADH *in vitro* shows autofluorescence lifetimes of around 0.4 ns, protein-bound NADH can show decay times of 1.2 up to 5 ns.[35] Time-resolved fluorescence lifetime imaging almost always aims to detect NADH, which is believed to be a sensitive method to investigate the redox state of tissue.[28,87–90] However, it has been discussed that a contribution of NADH to the FAF *in vivo* is unlikely, as its very short-wavelength fluorescence excitation maximum (350 nm) cannot be used in FAF imaging due to absorption by the lens and cornea.[16,91] Nevertheless, other studies describe autofluorescence lifetimes of ~1268 ps ($\tau_1 = 387$ ps, $\alpha_1 = 0.73$, $\tau_2 = 3650$ ps, $\alpha_2 = 0.27$ ps) upon an excitation at 446 nm.[15] Therefore, the effect of NADH on *in vivo* FLIO measurements should be further investigated.

The oxidized flavin FAD, located in mitochondria, is of interest regarding retinal fluorescence. Both FAD and FMN absorb light at 450-nm wavelength and show their maximal fluorescence emission at around 530 nm; reduced forms do not fluoresce under physiological conditions.[35,85] Typical autofluorescence lifetimes of these substances are 2.3 ns (FAD) and 4.7 ns (FMN), while protein-bound flavins show intermediate autofluorescence lifetimes (0.3 to 1 ns) with a weak fluorescence intensity due to quenching.[35] Skala et al.[21] determined the autofluorescence lifetime of protein-bound FAD to be 100 ps. *In vitro* FAF lifetime investigations show flavin decay times of around 2.4 ns.[15]

3.4 *Collagen and Elastin*

Different components of the extracellular matrix are found in the eye. Four different types of collagen as well as elastin were previously described and are likely fluorescent.[15,86,92–95] The collagens (I, II, III, and IV) emit fluorescence at ~510 nm (excitation 446 nm).[19] Time-resolved autofluorescence investigations show different lifetimes for each type of collagen (I: 1748 ps; II: 1435 ps; III: 1106 ps; IV: 1619 ps).[15] The autofluorescence lifetime of elastin was described to be 1279 ps.[15]

3.5 *Other Fluorophores*

The skin pigments melanin and bilirubin emit fluorescence at a maximum of 436 nm (melanin) and 520-540 nm (bilirubin).[15,96] As melanin occurs not only in the iris but also in the choroid and the RPE layer, it is of special interest when investigating FAF lifetimes. The excitation maximum of melanin, however, is at 360 nm. Excitations above 400 nm lead to a weak fluorescence signal. Nevertheless, time-resolved *in vitro* measurements at

446 nm excitation showed mean autofluorescence lifetimes of melanin powder at 916 ps ($\tau_1 = 280$ ps, $\alpha_1 = 70\%$; $\tau_2 = 2.4$ ns, $\alpha_2 = 30\%$).[15] Considerably shorter lifetimes were determined for melanin dissolved in PBS ($\tau_1 = 0.03$ ns, $\tau_2 = 0.62$ ns, $\tau_3 = 3.24$ ns).[97]

The aromatic amino acids tyrosine, phenylalanine, and tryptophan also fluoresce, but the excitation lies within the ultraviolet range (260 to 295 nm), and the emission maxima can be found between 280 and 350 nm.[35] Therefore, a fluorescence detection of these substances is unlikely with FLIO imaging.

Protoporphyrin IX, occurring within the cytochrome-c complex in mitochondria and as a byproduct in the synthesis of hemoglobin, shows fluorescence at an emission maximum of 635 nm, with an autofluorescence lifetime in the nanosecond range.[85] Its detection was discussed in relation with tumorigenesis, as the amount of protoporphyrin may increase in proliferative tissue.[36,98,99]

Pathological fluorophores, such as advanced glycation endproducts (AGEs), also show fluorescence at the retina.[15,100] They are discussed within the disease-related sections of this paper.

The lifetime of isolated RPE was determined as $\tau_m = 273.6$ ps ($\tau_1 = 210$ ps, $\alpha_1 = 0.96$, $\tau_2 = 1800$ ps, $\alpha_2 = 0.04$).[15]

4 Clinical Applications in Ophthalmology

4.1 *Healthy Eye*

FAF lifetimes of the healthy eye have thoroughly been investigated. The pattern of FAF lifetimes in a healthy eye was first described by Schweitzer et al.[15,28,39] using the first experimental device for ocular time-resolved fluorescence detection, which had a slightly different setup (e.g., an excitation laser of 446-nm wavelength). The group presented the fluorescence data of a healthy 25-year old subject analyzed with a triexponential approach. Here, very short τ_1 (150 ps) were found at the macular region and the longest τ_1 (>250 ps) were found at the optic disc.[15] Dysli et al.[40] focused on describing the parameter τ_m using a biexponential fit and found a very similar pattern with shortest τ_m at the macular center (SSC: 208 ps; LSC: 239 ps) and increasing values toward the peripheral retina. This study investigated patients aging from 22 to 61 years with a mean age of 35 years. FAF lifetime values were obtained from within the standardized early treatment diabetic retinopathy study (ETDRS) grid. The longest FAF lifetimes are found at the area of the optic disc. A third study describing the FAF lifetimes in healthy eyes in 2015 confirmed the same lifetime distribution pattern.[45] Here, a young group of patients with a mean age of 24 years (range: 21 to 35) was investigated and mean foveal τ_m were described to be very short (SSC: 82 ps; LSC: 126 ps).[45] Although the patterns are identical, the lifetimes differ between those two studies. This is easily explained by the use of two exponentials by Dysli et al.; however, by a three-exponential fitting of the decays by Sauer et al., FAF lifetimes appear to correlate significantly with age in non-dilated eyes.[40] Both spectral channels, but especially the LSC, seem to be influenced by an age-dependent effect.[40,45] The origin of this effect can only be speculated, and it may be found within the lens or the accumulation of lipofuscin, as the lipofuscin fluorescence signal seems to be predominantly detected in the LSC.[15]

In healthy eyes, FLIO always shows the same lifetime distribution patterns with the fovea showing the shortest FAF lifetimes. Figure 4 shows this typical pattern. A large part of FLIO-related research focused on describing the origin of these different decay times. *Ex vivo* investigations in porcine retinae showed shortest FAF lifetimes at the level of the RPE. Therefore, it was first believed that, also in human eyes, the RPE, containing melanin and lipofuscin, accounts for the short FAF lifetimes.[9,19,101] As fluorescence of MP was detected in Raman-based measurements, it was later speculated that MP might also have an influence on the autofluorescence lifetimes at the foveal center.[40,82] The impact of MP on short FAF lifetimes was carefully investigated in two further studies.[45,46] The first study, investigating a group of healthy young subjects, found a strong negative correlation of foveal FAF lifetimes with the amount of MP (SSC $r = -0.76$, LSC $r = -0.66$; $p < 0.001$).[45] The second study, confirming the hypothesis that short foveal autofluorescence decay times are strongly influenced by the MP, investigated a group of patients with macular holes.[46] Here, the MP is dislocated toward the side of the macular hole in a ring-shaped manner, and the short autofluorescence lifetimes are dislocated in the same way. After successful surgery, both MP as well as shortest FAF lifetimes relocated back toward the foveal center.[46] A recent study investigating macular carotenoids *in vivo* and *in vitro* confirmed these findings.[102] A thorough analysis of pigments in solution at different concentrations as well as their corresponding binding proteins was performed.[102] The autofluorescence lifetimes of carotenoids in PBS-CHAPS solution were found to be around 50 ps (lutein) and 60 ps (zeaxanthin). The respective binding proteins showed similarly short FAF lifetimes (around 40 to 50 ps). However, combining either carotenoid with their respective binding protein resulted in prolonged autofluorescence lifetimes (about 70 to 90 ps).[102] In a different review article, unpublished data were mentioned where autofluorescence lifetimes of lutein and zeaxanthin in solution measured with FLIO were found to show similarly short FAF lifetimes.[16] Although the fluorescence intensity of macular carotenoids is very low, MP impacts the *in vivo* FAF lifetimes, resulting in the short foveal fluorescence decay times.

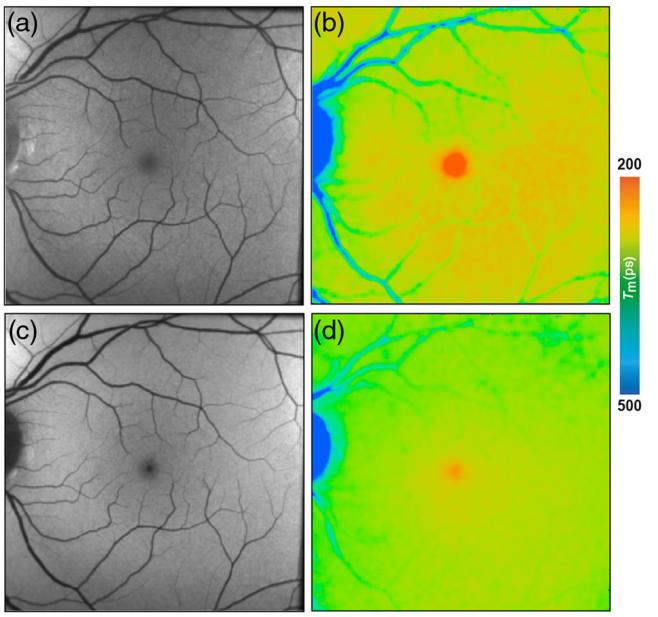

Fig. 4 (a, c) FAF intensity and (b, d) lifetime images from a 25-year-old healthy person. Images of (a, b) the SSC (498 to 560 nm) and (c, d) the LSC (560 to 720 nm) are presented.

Intermediate FAF lifetimes are found all across the human retina. It has been discussed that they most probably show the influence of lipofuscin from the RPE. These FAF lifetimes are similar to those found inside of macular holes, where the fluorescence signal comes from the RPE only.[46] Under physiologic conditions, an influence of the neuronal retina is possible as well.[15]

The longest FAF decays in healthy eyes are found at the optic disc. They have been attributed to connective tissue molecules, such as collagen and elastin.[15]

In general, the healthy pattern in FLIO investigations is reproducible and constant throughout literature. Although not every possible fluorophore at the retina has been thoroughly investigated, and only few studies focused on the longest FAF lifetimes, the general pattern of the healthy eye can now be explained.

4.2 *Albinism*

Patients with albinism often present with reduced foveal depression.[77,103–106] Their MP levels are typically low or not detectable, but the extent of measurable MP in albinism has been discussed diversely.[105,107,108]

Two patients with albinism were recently investigated with FLIO.[102] Figure 5 shows the FLIO images from a typical patient with albinism. In FAF intensity images, the fundus in these patients seemed to have normal autofluorescence with the exception of little to no MP absorbance. In FLIO imaging, no short FAF lifetimes were detected from the center of the fovea except for one eye with a little amount of MP. The authors suggest that FLIO may reliably show the actual amount of MP.

A previous study by Wolfson et al.[107] investigated MP in patients with albinism using with dual-wavelength autofluorescence imaging. Evidence for MP accumulation was reported in this study. Other reports did not confirm MP in patients with albinism.[105,108] Dual-wavelength autofluorescence imaging often shows a sloping baseline of MP, which may be a miscalculation due to the absence of melanin. This may therefore be a miscalculation commonly seen in measurements of patients with albinism, whereas FLIO can confirm that there is no MP measurable in these patients.[102] Nevertheless, this confirms again the impact of MP on the short FAF lifetimes at the fovea. In addition, as melanin is missing in patients with albinism, this could possibly be another cause of prolonged FAF lifetimes, not only in the fovea but also over the entire retina. A deeper penetration of the excitation light to the choroid is also possible; in that case, a higher contribution of fluorescence from collagen could be detected. Furthermore, Peters et al.[9] previously attributed shortest FAF lifetimes in the RPE of porcine eyes to the melanin. Thus, its lack also may result in longer fluorescence lifetimes. The impact of the missing melanin on the overall FAF lifetimes in human eyes *in vivo* still needs to be investigated, as such a study has not been conducted to this point.

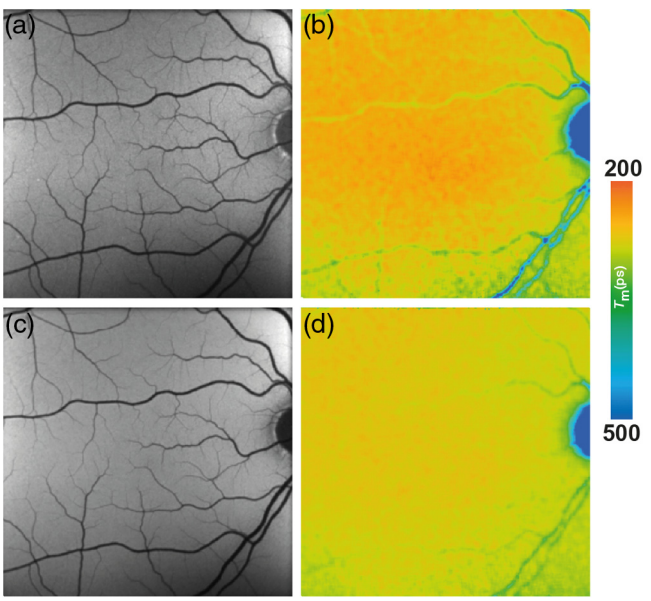

Fig. 5 (a, c) FAF intensity and (b, d) lifetime images from a 44-year-old patient with albinism. Images of (a, b) the SSC (498 to 560 nm) and (c, d) the LSC (560 to 720 nm) are presented.

4.3 *Age-Related Macular Degeneration*

AMD is a leading cause of blindness in the western world. Two forms of AMD have been described, the exudative (neovascular) and the nonexudative (dry) AMD.[109,110] A genetic risk is likely involved in the pathogenesis of the disease.[111–114] Clinically, both forms present retinal drusen (small yellowish deposits of metabolic byproducts), pigment disruption, and a thickening of Bruch's membrane. Neovascular AMD additionally shows subretinal or intraretinal fluid. Whereas exudative AMD can be treated with vascular endothelial growth factor antagonists (anti-VEGF), no sufficient treatment has been established for the nonexudative form yet.[115] Nevertheless, light-induced oxidative pathology might be reduced under carotenoid supplementation strengthening the MP, and AMD patients are likely to show reduced progression rates of the disease.[116–118] A connection between MP and visual function in AMD has also been described.[119] However, various studies have published discordant results, and no uniform recommendation on the supplementation of lutein and zeaxanthin has been made so far.[69,111,115,116,120–128] Both forms of AMD may lead to atrophy of the retina in their end-stages. The late stage of nonexudative AMD is called geographic atrophy (GA), and literature uses the term "macular atrophy" in cases of advanced exudative AMD.[129,130]

Fluorescence-based retinal imaging modalities, especially FAF intensity imaging, appear to be helpful in AMD diagnostics.[131–134] The disease has also been intensively investigated with FLIO, starting in 2004 when Schweitzer et al.[15,39,135] found altered FAF lifetime patterns within patients with AMD. In a study investigating 15 patients with AMD, a prolongation of different FAF lifetime components was found even in early stages.[101,135] This study was performed with an early experimental device, and, as the Heidelberg FLIO became available, more studies with increased patient numbers were conducted.[43,44,50,136]

FAF lifetimes in patients with AMD are generally prolonged as compared with healthy controls. This holds true for exudative as well as nonexudative AMD.[16,44,136] A recent study from Salt Lake City showed that there was no significant differences in the central area of a standardized ETDRS grid between AMD patients and age-matched controls (SSC: AMD: 196 ps, healthy: 210 ps, $p = 0.39$; LSC: AMD: 299 ps, healthy: 284 ps, $p = 0.29$), whereas the outer ring of that same grid showed highly significant differences between both groups (SSC: AMD: 342 ps, healthy: 313 ps, $p < 0.001$; LSC: AMD: 403 ps, healthy:

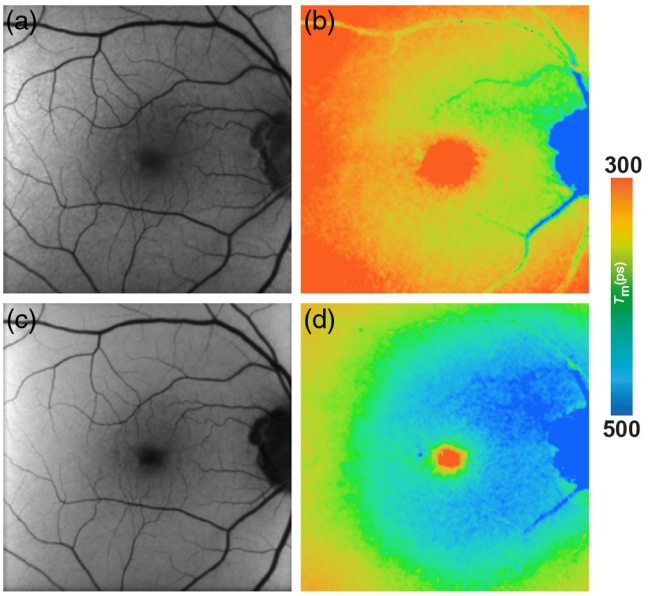

Fig. 6 (a, c) FAF intensity and (b, d) lifetime images from a 73-year-old patient with AMD. Images of (a, b) the SSC (498 to 560 nm) and (c, d) the LSC (560 to 720 nm) are presented.

340 ps, $p < 0.001$). The FLIO group from Bern similarly reported a prolongation in the outer ring of the ETDRS grid and additionally distinguished between phakic and pseudophakic eyes (Phakic patients: SSC: AMD: 613 ps, healthy: 346 ps, $p < 0.0001$; LSC: AMD: 545 ps, healthy: 370 ps, $p < 0.0001$; pseudophakic patients: SSC: AMD: 404 ps, healthy: 325 ps, $p < 0.001$; LSC: AMD: 475 ps, healthy: 419 ps, $p < 0.05$). Differences in the absolute numbers may be caused by different inclusion criteria, especially the exclusion of eyes late dry AMD and neovascular AMD from statistical analysis in the study conducted at Salt Lake City. Another difference lies within the calibration difference among the different cameras. Nevertheless, both groups find prolongations of mean FAF lifetimes in the outer ring of the standardized ETDRS grid. The prolongation of mean FAF lifetimes seems to be especially pronounced within the LSC and may be an early sign of the bis-retinoid accumulation within the RPE.[16] In early stages of AMD, metabolic changes may occur before they are visible in conventional imaging techniques.[137] The recent FLIO study gives hints that these metabolic alterations may be detectable with this technique, as a typical and likely AMD-associated pattern of prolonged FAF lifetimes was found.[136] This pattern is ring-shaped, presents between the large vessels with a diameter ~3 to 6 mm centered at the fovea, and is most pronounced in the LSC.[136] Figure 6 shows the pattern, which was found in all 150 eyes with nonexudative AMD investigated in the study. It was described to be most prominent in the superior and nasal area. Furthermore, the authors believe that this pattern progresses over time and may thereby indicate the disease progression as well.[136] A significant difference in the pattern has been described in the area of the outer ring between early and intermediate AMD ($p < 0.05$), whereas the central area did not show significant differences between different disease stages ($p = 0.4$).[136] Longitudinal studies are in progress. Furthermore, 36% of the age-matched controls showed that pattern as well, many of which showed small drusen (<63 μm), or had a highly positive family history of AMD. The authors believe that this trace pattern may be indicative of a high risk to develop AMD in eyes that are still considered healthy.[136] Future research should be directed toward long-term follow-up investigations of these changes.

Intraretinal fluid from neovascular AMD, however, does not seem to significantly influence the mean FAF lifetimes.[16] Further changes of FAF lifetimes were caused by intraretinal and subretinal deposits as well as atrophic processes. The next paragraphs focus on these conditions.

Drusen were first described in 1855 and are yellowish deposits that can be seen funduscopically.[138] They represent extracellular debris deposits and are located between the basal lamina of the RPE and Bruch membrane's inner collagenous layer.[111,139] Chronic inflammation caused by cellular remnants and debris as well as complement dysregulation seems to play a role in their development.[137,140–142] From clinical appearance, AMD can be classified according to the Beckman Initiative for Macular Research Classification Committee as early (medium drusen, 63 to <125 μm), intermediate (confluent drusen >125 μm, pigmentary changes), and late (GA) AMD and showing different drusen types: soft, intermediate, and hard drusen, cuticular drusen, crystalline drusen, refractive, and reticular pseudodrusen.[143] Although there are many different diseases in which drusen may occur, and even the normal aging fundus may show some drusen, they are a typical hallmark of AMD.[111,137]

One recent FLIO study especially focused on drusen in AMD.[44] Here, FAF lifetimes of soft drusen as well as reticular pseudodrusen were analyzed. FAF lifetimes of both deposits showed a broad range of autofluorescence lifetimes and were on average not significantly different from the surrounding retina. Drusen, although often appearing hyperfluorescent in FAF intensity images, were not directly identifiable with FLIO.[44] The relatively short autofluorescence from the RPE may also be blocked, which may also be the cause of prolonged FAF lifetimes in AMD.[16,137] This was thought to reflect an increase of connective tissue in the remodeling process of the disease at the level of the RPE-photoreceptor band.[16,44] Previous *ex vivo* studies found significantly prolonged FAF lifetimes in extramacular drusen as compared with the surrounding RPE.[37] Another recent article focusing on AMD changes *in vivo* reveals information about drusen, where all investigated drusen types (soft, hard, and pseudodrusen) showed significantly prolonged FAF lifetimes as compared with the adjacent retina when conducting a paired sample *t*-test.[136] In contrast to the previous, drusen-based article, no shortening of FAF lifetimes in the area of drusen was found.[44,136] The authors attribute this to the specific inclusion of nonexudative AMD only, whereas the previous study included both AMD types. Short FAF lifetimes in the area of drusen may therefore be associated with neovascular AMD.

The development of GA, the late stage of dry AMD, may also be related to RPE drusen patterns.[144–146] While both the etiology as well as prognostic factors of GA are still under investigation, retinal imaging may be important for a better understanding of the disease. Areas of atrophy often spare the fovea initially, but they eventually progress and cause central vision loss.[130,144,146–148] The progressive atrophy involves the choriocapillary and RPE layer as well as the outer retina.[130,149] Bindewald et al.[131] graded different appearances of GA and also classified the fovea as affected or spared.

So far, two studies investigated GA with FLIO.[43,50] FAF lifetimes from atrophic areas were described to show a broad range of much prolonged FAF lifetimes.[43,50] This was discussed as

a missing contribution of short fluorescence lifetimes from the RPE, an increase of connective tissue, and a larger contribution of long fluorescence lifetimes from the choroid. Short FAF decays were sometimes still detected in the foveal center, which originate from persisting MP.[43,50] This may hint foveal sparing. As GA lesions within the fovea are difficult to identify due to the presence of fluorescence-intensity blocking MP, FLIO may be able to help in the prediction of spared versus nonspared fovea.[149]

In addition, the marginal zone of GA, which seems to play a role in disease progression, can be analyzed with FLIO. Furthermore, FLIO may be useful for monitoring the disease progression as the border zone of the atrophy can be analyzed.[43,50] Nevertheless, further follow-up studies need to be conducted to investigate if altered FAF lifetimes in these areas may in fact be related with disease progression. It might also be interesting to monitor the effect of novel treatment options, such as complement factor inhibitors, with FLIO.

4.4 *Diabetic Retinopathy*

Retinal microangiopathy is a common complication of diabetes.[150] It leads to inflammatory processes at the neuronal level, retinal degeneration, and disturbances at the blood–retina barrier as well as macular edema.[151,152] Hyperglycemia, as the primary event in diabetes, causes general protein glycation as well as a formation of AGEs. This may lead to endothelial dysfunction and disturbance of the protein kinase C pathway.[151,153] AGEs may play an important role in the pathogenesis of DR, as their concentration in serum was found to increase with severity of DR.[154] They are fluorescent molecules, and an increase in FAF intensity has been found in studies on diabetic macular edema.[155,156]

Multiple studies investigated time-resolved FAF in patients with diabetes.[47,101,157] Figure 7 shows the FLIO image of a patient with DR. The FAF lifetimes in patients with DR appear to be generally prolonged. In a first study, Schweitzer et al.[101] compared patients with DR with age-matched healthy controls. The shift to longer fluorescence decays was discussed as a sign of reduced oxidative metabolism, an increased contribution of protein-bound NADH as an effect of glycolysis, and the accumulation of AGEs. Schweitzer et al.[157] also speculated about detecting prolonged FAF lifetimes from the crystalline lens, as AGEs also appear in the lens. A further study analyzed FAF lifetimes from a group of 48 type 2 diabetes patients, which had clinically no signs of DR. These were compared with an age-matched group of 48 healthy controls. Although the fundus appeared healthy in OCT imaging and fundus photography, FLIO seemed to show early metabolic alterations in terms of a general prolongation of FAF lifetimes. Although it was not possible to assign specific fluorophores to cause these alterations, the above-mentioned pathological mechanisms and especially the accumulation of AGEs were discussed again.[157] In a subgroup analysis, the authors were able to discriminate diabetic patients from healthy controls much better in phakic than in psudophakic subjects. Based on this, they assumed an influence of AGEs-accumulation in the crystalline lenses of diabetic patients.[157]

A more recent study investigated a group of patients with DR.[47] FAF lifetimes from different regions of interest in 34 patients with nonproliferative diabetic retinopathy were compared with age-matched healthy controls.[47] The results were consistent with previous studies, and increased FAF lifetimes were recorded in the patient group for all regions of interest. This was more pronounced in the SSC, where the crystalline lens has a larger impact. The formation of AGEs was discussed again as the main reason for the prolongation of autofluorescence lifetimes.[47]

These investigations show consistent results and indicate that FLIO has the potential to detect metabolic alterations at very early disease stages. Such alterations may be caused by the accumulation of AGEs as well as disturbances within the coenzymes of cellular metabolism in diabetic conditions.

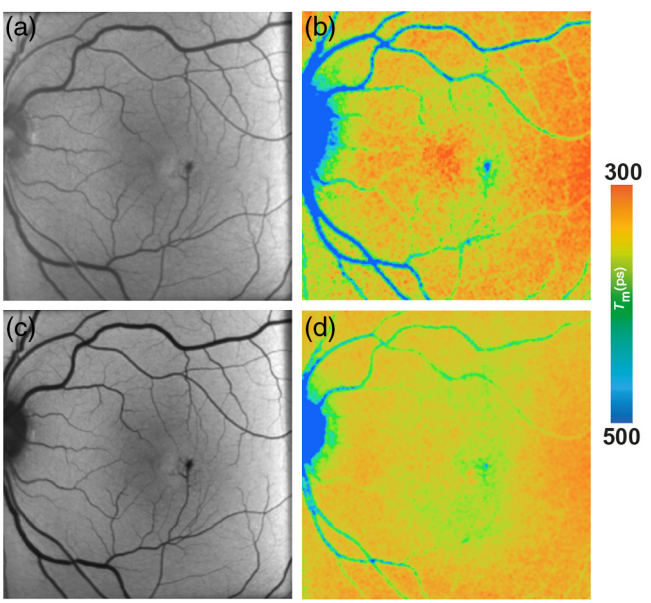

Fig. 7 (a, c) FAF intensity and (b, d) lifetime images of the SSC (498 to 560 nm) from a 63-year-old patient with DR. Images of (a, b) the SSC (498 to 560 nm) and (c, d) the LSC (560 to 720 nm) are presented.

4.5 *Macular Telangiectasia Type 2*

MacTel is an uncommon retinal degenerative disease usually showing a late onset around the sixth life decade. However, earlier onsets are described in literature with the youngest MacTel patient being diagnosed at the age of 21.[48] The disease results in vascular and neurodegenerative changes and central vision loss.[158–163] Changes occur within the so-called MacTel area, with an extension of 5 deg vertically and 6 deg horizontally, with the fovea in its center. A dominant genetic inheritance with reduced penetrance is likely, and the glycine/serine pathway may play a key role. So far, no specific gene has been found.[164–168] MP levels change during the course of the disease. They show very low levels and an accumulation in a ring-shaped manner around MacTel area.[77,102,169–175]

At this point, there is no treatment of MacTel available, and intravitreal injections of steroids or anti-VEGF have not been successful,[176–178] but ciliary neurotrophic factor may be beneficial and is currently being investigated. Therefore, the call for a reliable imaging modality to diagnose the disease at early stages is increasing.[179] In ophthalmologic examinations, a retinal graying is described, and OCT imaging often shows temporal cysts. It is believed that the prevalence of MacTel is underestimated, as it is often mistakenly classified as exudative AMD.[180,181] Reliable diagnosis based on retinal imaging is especially difficult at early stages of the disease, and there is no gold-standard

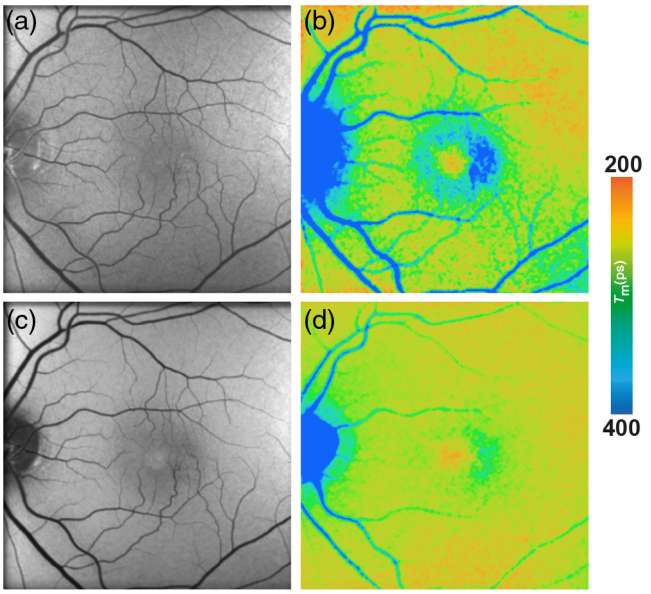

Fig. 8 (a, c) FAF intensity and (b, d) lifetime images from a 58-year-old patient MacTel. Images of the (a, b) SSC (498 to 560 nm) and (c, d) the LSC (560 to 720 nm) are presented.

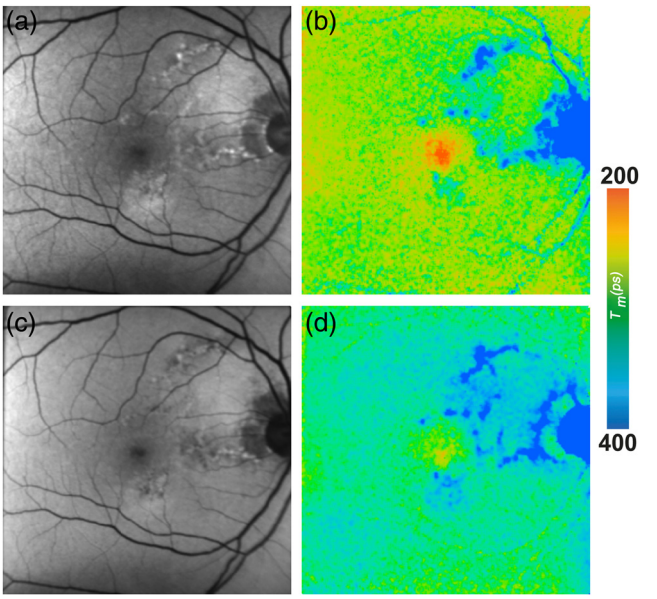

Fig. 9 (a, c) FAF intensity and (b, d) lifetime images from a patient with a BRAO. Images of (a, b) the SSC (498 to 560 nm) and (c, d) the LSC (560 to 720 nm) are presented.

imaging modality yet. Blue-light reflectance imaging as well as fluorescein angiography appeared helpful, but other imaging modalities also were discussed.[178,182–188]

FLIO images show very distinct changes at the area of the MacTel zone, as τ_m prolongs in a crescent-shaped manner temporal to the fovea in early stages. In more advanced stages, FAF lifetimes of the entire MacTel area are shifted to longer means in an oval-shaped manner.[48] This is shown in Fig. 8. The temporal area of the inner ring from a standardized ETDRS grid (T1) was used to describe the MacTel-related changes, the temporal area of the outer ring (T2) was used as a reference. The nasal area from the inner ring of a standardized ETDRS (N1), as well as the central area from a standardized ETDRS grid (C), was also investigated. In eyes with MacTel, T1 was significantly longer than the other investigated areas (T1: 382 ± 81 ps, T2: 312 ± 69 ps, C: 313 ± 68 ps, N1: 355 ± 73 ps).[48] In healthy eyes, however, T1 was significantly shorter than N1, and slightly shorter than T2 (T1: 298 ± 84 *ps*, T2: 301 ± 73 ps, C: 220 ± 81 ps, N1: 312 ± 48 ps).[48] A T2/T1 ratio below 0.9 indicates that a patient is likely affected with MacTel.[48] In addition, the MacTel-related MP changes can also be monitored with FLIO.[48,102] In early stages of the disease, MP can show nearly normal levels with a central peak. In these cases, short central autofluorescence lifetimes are present as well. In the course of the disease, MP may enhance in an oval-shaped manner surrounding the MacTel zone. In these cases, the short autofluorescence decays can be found exactly in this area.

The changes within the FLIO signals, especially the temporal prolongation of τ_m, are visible at early stages of the disease and can be distinguished very well from AMD-related patterns. Therefore, FLIO opens new possibilities for reliable imaging and early diagnosis of MacTel.[48]

4.6 *Retinal Artery Occlusion*

Central artery occlusions (CRAOs) can be distinguished from peripheral branch retinal artery occlusions (BRAOs) clinically. They usually manifest as painless sudden vision loss.[189] There may be a slight visual impairment after CRAO, but often visual acuity remains considerably reduced.[190] In the acute phase of CRAOs, the retina is swollen, vessels appear attenuated, and the fundus appears pale with a red spot at the macular area as there is no retinal swelling at the fovea. After this phase of retinal thickening due to a shortage of oxygen in the acute stage of CRAO, all retinal layers are reduced in thickness measured with OCT.[191] The thickness of especially inner and middle retinal layers is described to remain reduced late after CRAO.[192]

First time-resolved fluorescence examinations in retinal artery occlusions were conducted with an experimental setup and published by Schweitzer et al.[101,193] Of special interest were BRAOs, as in these eyes perfused and nonperfused areas could be compared. CRAOs were investigated as well. The nonsupplied areas funduscopically appeared pale and the fluorescence intensity was low, resulting in hypofluorescent (dark) areas in FAF intensity images. The corresponding FAF lifetimes were much prolonged. Based on the different fluorescence signals, the authors also discussed the possibility of fluorescence signals originating from the neuronal retina.[101,193]

Typical FLIO images from one patient with BRAO are shown in Fig. 9. A more recent study to monitor changes in CRAO was published by Dysli et al.[41]; here, the current Heidelberg FLIO device was used. The results of this study are in accordance with previously published results. Twenty-four patients were included and imaged in the acute stage of CRAO (<3 days after vision loss). A significant prolongation of mean FAF lifetimes in the acute stage was found. This prolongation affected all areas of the standardized ETDRS grid, and the inner ring showed prolonged mean FAF lifetimes by 59% (209 ps, SSC) and 22% (89 ps, LSC) as compared with age-matched healthy eyes.[41] In contrast to previous studies, which presented only cross-sectional investigations, the patients were followed up by Dysli et al. and imaged again in the postacute stage (>30 days after vision loss). Here, the inner retinal layers of previously nonsupplied areas developed atrophy. However, FAF lifetimes were found to be comparable

to those of the unaffected fellow eyes.[41] The authors came to the conclusion that hypoxia and swelling of the inner retinal layers influence and prolong the measured mean fluorescence lifetimes.[101] However, the fluorescence signal of thinned retinal layers was comparable to retinal layers of normal thickness in a healthy retina.[41]

Ischemic conditions change the microenvironment in human tissue, such as the pH values, ionic states, enzymatic activation, inflammation, and the increased formation of reactive oxygen species.[194–197] In addition, the coenzymes of cellular energy metabolism may change when oxygen is lacking. These conditions were also discussed previously.[16,41] Briefly, due to a lack of adenosine triphosphate in acute hypoxia, the redox pairs NAD+/NADH (oxidized and reduced NADH) as well as FAD/$FADH_2$ (oxidized and reduced FAD) could also be affected. In particular, NADH and FAD bound to certain proteins emit fluorescence signals.[84] It was discussed that it is unlikely that the fluorescence of NADH significantly affects the FAF lifetimes measured with FLIO, as NADH shows excitation and emission spectra of very short wavelengths, and therefore this fluorescence signal *in vivo* is likely blocked by the lens and cornea.[41] The fluorescence characteristics of FAD are within the detectable range of FLIO (excitation maximum: 450 nm; emission maximum: 528 nm).[198] In particular, the hypoxia-induced shift from protein-bound FAD with short autofluorescence lifetimes to reduced $FADH_2$ (with either no or extremely weak autofluorescence at longer autofluorescence decay times) might influence the FAF lifetime signal.[41] In addition, blockage from inner retinal swelling may further reduce the short FAF signal from the RPE, prolonging FAF lifetimes in acute stages even more.[199]

Ultimately, retinal artery occlusions show the consequences of acute lack in the supply of oxygen very well and therefore present an *in vivo* model of retinal ischemia.

4.7 *Stargardt Disease*

The common and most prevalent single-gene inherited retinal dystrophy called Stargardt disease leads to a progressive loss of the central vision.[200,201] Usually within the second decade of life, the mutation in the ABCA4 gene manifests with symptoms, rendering most patients legally blind by the third life decade.[202] The ABCA4 gene codes for the ABCA4 transmembrane transporter, which belongs to a group of ATP-binding cassettes (subfamily A) and is almost exclusively found in the photoreceptor outer segments in the human retina. Here, it plays a role in the transport of vitamin A derivatives originating from the visual cycle. Mutations in this gene lead to a degeneration of photoreceptor outer segments and consecutive RPE cell death caused by the accumulation of bis-retinoid adducts of all-*trans*-retinal, lipofuscin, and other by-products from the visual cycle.[203–207] Usually, patients in early stages present a generally increased FAF intensity with normal photoreceptor function.[206] Later, yellowish spots of deposits appear across the fundus, which finally result in retinal atrophy. These spots initially appear as hyperfluorescent in FAF intensity. In later stages, the FAF intensity is reduced, correlating to an absence of the RPE cell layer in atrophic areas.[208,209] Various pharmaceutical approaches have been summarized to reduce the accumulation of visual cycle by-products and to slow down the development of retinal atrophy.[210,211] It has also been found that higher peripheral levels of retinal carotenoids can be correlated with reduced amounts of A2E in the RPE.[121] As therapeutic approaches are progressing, the need for imaging modalities for detection of disease progression at early disease stages is rising.[211,212]

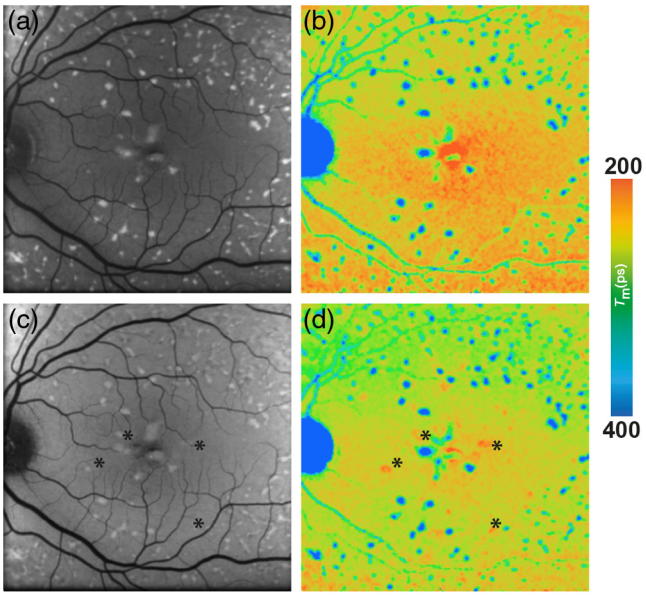

Fig. 10 (a, c) FAF intensity and (b, d) lifetime images from a 48-year-old patient with Stargardt disease. Images of (a, b) the SSC (498 to 560 nm) and (c, d) the LSC (560 to 720 nm) are presented. * highlight different flecks.

In one FLIO-related study, 16 patients with Stargardt disease were monitored.[42] Dysli et al. found that hyperfluorescent flecks can show both prolonged (474 ps) as well as shortened (242 ps) FAF lifetimes as compared with the normal retina (322 ps). FAF lifetimes of unaffected retinal structures (without deposits or atrophy) were comparable to those of age-matched healthy individuals. Follow-up examinations showed a shift of flecks with shortened FAF lifetimes to longer values over time. The authors discussed this as a change of composition within these deposits. Based on *ex vivo* findings, they attributed the short FAF component to compounds in the degenerating photoreceptor cells, especially retinaldehyde adducts and bis-retinoid fluorophores.[42,213] Longer FAF lifetimes were attributed to photodegenerated products of A2E. Dysli et al.[42] also found that flecks of short FAF lifetime appeared even before hyperfluorescence was detectable in FAF intensity imaging. Figure 10 shows a patient with Stargardt disease showing such flecks. FLIO is therefore a very promising tool in the investigation and imaging of Stargardt disease and its progression. It might also prove to be very helpful in detecting and monitoring therapeutic effects.

4.8 *Central Serous Chorioretinopathy*

CSCR mostly affects young, white male patients (typical age range: 20 to 50 years).[214] It is associated with focal leakage of fluid through the RPE at the macular area, leading to a detachment of the neurosensory retina and a decrease in visual acuity. In most cases the fluid resolves spontaneously, and patients often retain good visual acuity of 20/30 or better.[214–216] However, there are chronic forms with persistent or recurrent subretinal fluid.[217] This can result in atrophy of the RPE and permanent vision loss. Different risk factors for the development of the disease were identified, such as hypertension, steroid usage, sleep disturbances, *Heliobacter pylori* infections, autoimmune diseases, and various others.[218] Nevertheless, the

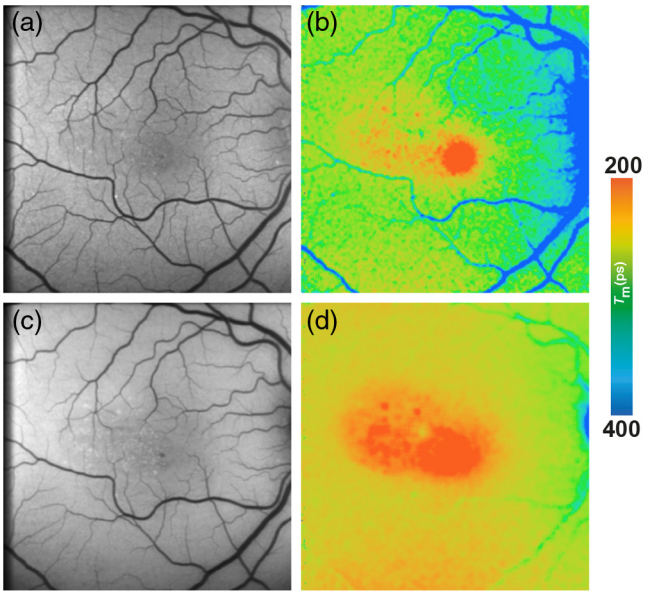

Fig. 11 (a, c) FAF intensity and (b, d) lifetime images from a 33-year-old patient with CSCR. Images of (a, b) the SSC (498 to 560 nm) and (c, d) the LSC (560 to 720 nm) are presented.

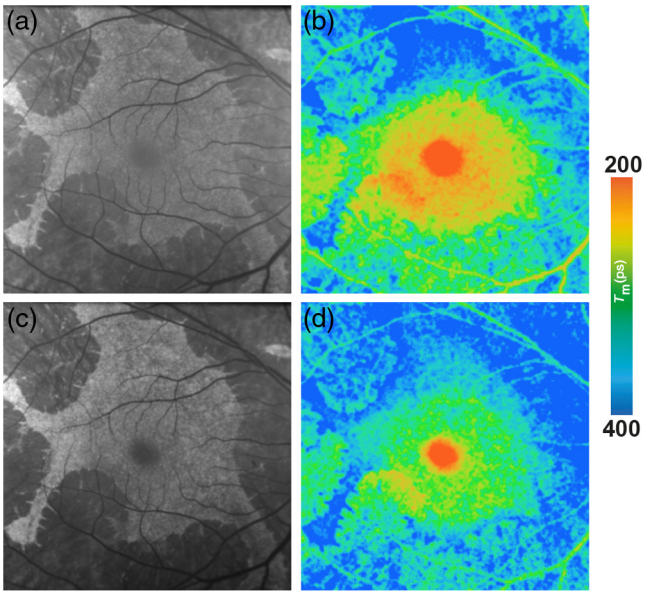

Fig. 12 (a, c) FAF intensity and (b, d) lifetime images from a 18-year-old patient with choroideremia. Images of (a, b) the SSC (498 to 560 nm) and (c, d) the LSC (560 to 720 nm) are presented.

pathophysiological conditions underlying the disease are currently still under investigation.[214,219]

FLIO was performed on 35 patients with CSCR in different stages of the disease.[49] Representative images are shown in Fig. 11. Affected areas in patients with an onset of symptoms under 6 months previous to investigation presented shorter mean autofluorescence decay times in affected eyes as compared with healthy control individuals.[49] The inner ring of a standardized ETDRS grid showed a shortening of mean FAF lifetimes by 15% in the short and by 17% in the long spectral channel compared with healthy control eyes [inner ring: 216 ± 8 ps (SSC) and 235 ± 6 ps (LSC)]. A $P < 0.01$ and $P < 0.0001$, respectively, were reported. Similarly shortened lifetimes were reported for the outer ring as well as the central area of the standardized grid.[49]

These short FAF lifetimes appeared to correlate with an elongation of photoreceptors, which could be due to the accumulation of visual cycle by-products.[59,220] Shortened FAF lifetimes in FLIO measurements as a result of the accumulation of bisretinoids, and other by-products were also discussed for other retinal diseases.[42] Over time, FAF lifetimes appeared similar to the healthy retina, and secondary retinal changes (atrophy or scar formation) resulted in prolonged FAF lifetimes in CSCR patients.[49] The processes here are probably comparable to the formation of GA in AMD, where long FAF lifetimes were assigned to components of the connective tissue.[43,50] Similar to other FLIO-based studies, subretinal fluid (present or absent) did not seem to influence FAF lifetimes.[49]

4.9 *Choroideremia*

Choroideremia is a rare, X-linked recessive inherited retinal disease, affecting approximately 1 in 50,000 males. This monogenic disease affects the CHM gene, coding for the Rab escort protein-1, which takes part in membrane trafficking in the retina and RPE. Choroideremia leads to progressive vision loss and ultimately results in blindness. It affects different retinal layers, such as the neurosensory retina, the RPE, and the choroid.[221] Viral vectors were designed recently to replace the mutated genes, and related research is still actively ongoing.[222] Distinct autofluorescence patterns were found in FAF intensity imaging, where the area of remaining autofluorescence seems to inversely correlate with the progression of the disease.[223]

FLIO was performed on 8 patients (16 eyes) with advanced choroideremia.[224] FLIO images provided more information on atrophy of specific retinal layers including RPE than simple FAF intensity measurements. Hereby, individual areas of different atrophic stages were clearly separable from another.[224] Areas with complete chorioretinal atrophy showed very long mean FAF lifetimes (SSC: 1116 ± 63 ps, prolonged by 364% compared with healthy controls; LSC: 915 ± 52 ps, prolonged by 270% compared with healthy controls). However, in areas of RPE atrophy where photoreceptor layers were still persistent (verified by OCT), shorter FAF lifetimes were found (SSC: 567 ± 59 ps; LSC: 603 ± 49 ps), compared with the areas where the photoreceptors were lost (see FAF lifetimes above).[224] Intact retinal layers at the macula area showed the shortest mean FAF decay times. Figure 12 shows these findings. As discussed previously, these short FAF decay times likely originate from accumulated by-products of the visual cycle and possibly even show a persistent activity within the visual cycle.[225] Follow-up examinations showed a correlation of disease progression with increase of chorioretinal atrophy and decreasing areas of short fluorescence lifetimes.

4.10 *Retinitis Pigmentosa*

RP is a degenerative retinal disease that can be protracted with little progression over decades or that can escalate to legal blindness in a matter of years.[226,227] Indeed, RP could be considered an umbrella diagnosis, with a unified clinical picture and a vast number of etiologic causes. At least 79 different genes that contribute to proper retinal function have been shown to be mutated in RP.[228,229] In addition to having many causes, RP has diverse modes of inheritance with about 30% to 40% being autosomal dominant, 50% to 60% autosomal recessive, and 5% to 15%

X-linked.[226] Although age of onset and presenting symptoms vary, RP advances to a characteristic progressive peripheral loss of vision that is preceded by nyctalopia.[230,231] Central vision generally remains intact with tunnel visual fields that constrict over time.[232] Even before patients become symptomatic, photoreceptors decrease in function, and, over the course of the disease, the RPE undergoes atrophy resulting in vision loss.[233,234]

Two recent studies focus on describing FAF lifetimes in RP, showing a specific disease-related pattern.[235,236] Areas of peripheral atrophy (RPE and photoreceptor atrophy) can be identified showing very prolonged FAF lifetimes. In the LSC, FAF lifetimes of 401 ps were described for atrophic areas, compared with 282 ps of the same area in healthy subjects ($p < 0.001$).[236] However, areas with remaining photoreceptors in areas of RPE atrophy were found to show only slightly prolonged FAF lifetimes (301 ps in RP, compared with 263 ps in healthy subjects, LSC). Ring-like structures were investigated in both of these studies, showing good correlations with functional imaging and visual acuity.[235,236] Specifically, FLIO confirms prior FAF intensity imaging studies that describe a parafoveal hyperfluorescent ring in RP with coincident peripheral hypofluorescence indicative of retinal atrophy.[237] These rings shrink over time, corresponding to RP disease progression.[238] Both studies showed that central areas of short FAF lifetimes corresponding to MP remain relatively unaffected in RP, a finding consistent with the natural disease progression. Shorter FAF lifetimes in the foveal center correlated with better visual acuity.

Furthermore, one of the studies suggests that FLIO may be useful in better characterizing phenotypic patterns in various genetic subtypes of RP.[236] Hyperfluorescent rings appear as an area of generally short lifetimes with overt long lifetimes in peripheral atrophic regions. Figure 13 shows a typical patient with RP. Notably, inheritance-dependent phenotypic variance, related to the prominence of the ring-like pattern in RP, was found. Fundus FLIO images of patients with autosomal dominant RP and Usher syndrome displayed strong ring-like patterns, those with autosomal recessive RP a milder pattern, and those with X-linked RP no ring-like pattern at all.

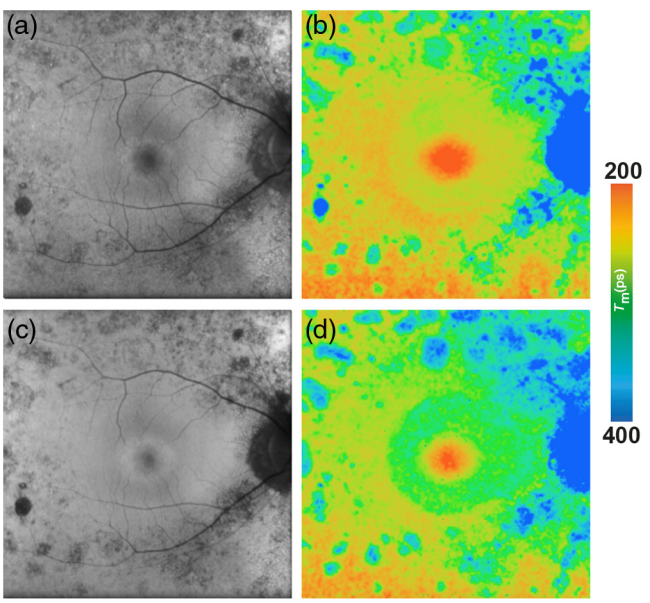

Fig. 13 (a, c) FAF intensity and (b, d) lifetime images from a 45-year-old patient with RP. Images of (a, b) the SSC (498 to 560 nm) and (c, d) the LSC (560 to 720 nm) are presented.

Overall, FLIO may give additional insights about the integrity of the retina and may be used in the future to shed light on genetic differences in the pathology and pathogenesis of various etiologic subtypes of RP. Although the presented studies were of a cross-sectional nature, it was suggested that longitudinal studies may demonstrate the usefulness of FLIO in monitoring disease progression of RP.[235,236]

4.11 *Alzheimer's Disease*

In a small pilot study, Jentsch et al.[51] investigated if Alzheimer's disease may cause changes in the FLIO signal. Here, the eyes of 16 patients were investigated. FAF lifetimes were investigated and correlated to Alzheimer-specific diagnostic markers obtained through lumbar puncture. Amyloid-β (1-42), total-tau-protein, and phosphorylated tau-181 (p-tau181) protein were investigated. This study was also performed with the early experimental device, before the Heidelberg FLIO became available. The results of this study indicate that the signal observed with FLIO correlates with the cognitive status (MMSE score), as well as the p-tau181 in the CSF.[51] These findings may indicate that FLIO holds the potential to detect early metabolic changes in Alzheimer's disease. At the recent ARVO meeting in 2018, Kwon et al. presented data from a more recent study investigating seven patients with cognitive impairment related to Alzheimer's disease and eight healthy subjects with FLIO.[239] They reported a correlation of Aβ and tau levels to FLIO parameters in phakic subjects only. Overall, the group sizes in each study were extremely small, and no control group was investigated in the pilot study. Therefore, these promising findings need to be thoroughly investigated in a larger and if possible longitudinal study before true assumptions can be made. Nevertheless, FLIO may eventually prove to be an approach in the noninvasive imaging of Alzheimer's disease.

5 Mouse Models

In the living eye, fluorescence lifetimes are measured within a complex system. Contribution of different retinal layers, cell types, molecules, molecular interaction, and pathways is expected. Thereby differentiation and isolation of fluorescence lifetimes of specific molecules and processes of interest prove challenging.

To investigate specific retinal conditions as well as degeneration processes, the FLIO technique has been established for the use in small rodents, especially in the mouse model by Dysli et al.[240] For a detailed summary, we refer to the recently published review article about FLIO and the corresponding fundamental publications.[16]

Dysli et al.[240] compared retinal fluorescence lifetime of pigmented (C57BL/6) and nonpigmented albino (BALBc) mice. Thereby, they found shorter mean fluorescence lifetime in nonpigmented compared with pigmented mice and proposed a correlation to the amount of melanin, which showed relatively long fluorescence lifetimes when measured *in vitro*. In contrast to the steady increase of fluorescence lifetimes in the human retina with age, fluorescence lifetime in the murine retina was shown to decrease over time and finally reach a similar mean lifetime value. In addition, Dysli et al. investigated a mouse model of slow retinal degeneration (short RDS, C3A.Cg-Pde6b^{+}Prph2^{Rd2}/J). Here, patchy changes of fluorescence

lifetimes were observed, mirroring the different stages of retinal degeneration within the same eye.[240]

To differentiate the contribution of different retinal layers to the measured mean autofluorescence lifetime, Dysli et al.[241] pharmacologically induced retinal degeneration. Sodium iodate ($NaIO_3$) was used for degeneration of the RPE followed by subsequent loss of photoreceptors.[242] On the other hand, specific degeneration of photoreceptors with preservation of the RPE was induced using N-methyl-N-nitrosourea.[243,244] Over the duration of the experiment of 1 month, a prolongation of the mean fluorescence lifetimes was observed in the absence of the RPE. However, if the RPE was preserved and only the photoreceptors were targeted and destroyed, shorter fluorescence lifetime values were measured.

Thereby, Dysli et al. concluded that short fluorescence lifetimes in the murine retina might originate from the RPE and might be influenced and modulated by the overlying neurosensory retina, which is in concordance with previous findings Ref. 9. In the absence of the RPE and the photoreceptors, increased contribution of other retinal layers such as the choroid might be detected, featuring relatively long fluorescence lifetimes.

As in ophthalmology, a separate mouse model exists for nearly all retinal conditions, disorders, and diseases; the FLIO technique in mice holds a versatile potential for future investigations in this field to characterize retinal changes, natural courses of disease, induced retinal changes, and potential therapeutical interventions in a standardized and well-controlled experimental setup.

6 Limitations

Although the observed changes in FAF lifetimes in different retinal diseases include many promising results, some limitations must be mentioned. At the current point of time, FLIO is still a research prototype. Therefore, it is not yet commercially available and the data presented here are from a few individual research sites only. We hope that FLIO will be available to a broader field of researchers and clinicians in the future, so studies can be conducted on a larger scale. Similarly, individual devices still differ due to a different calibration. Therefore, individual lifetimes often show small (device-dependent) differences. This is in large part due to the individual prototypes, and we strongly believe that this issue will be resolved in the near future. Nevertheless, looking at different FAF lifetime patterns, which can be found in different diseases, results among different research groups are comparable. Therefore, a multicenter investigation with FLIO is already possible to some extent. More research should be focused on finding data points that are comparable between individual centers.

Although the FLIO uses confocal optics, FAF lifetimes show a mixture of many fluorophores, likely from different individual layers of the fundus. In addition, the autofluorescence of the lens is very strong and cannot be completely blocked from FAF lifetime images.[245] By looking not at absolute numbers but at ratios or differences within one eye, this problem can be minimized. Nevertheless, a data analysis approach, possibly excluding lens autofluorescence from the measurement, would be extremely helpful. In comparison with measurements in reflection, the suppression of the light originating from the anterior part of the eye by the confocal principle is considerably reduced in autofluorescence measurements. In the published studies, the subjects have had clear ocular media. Also, in these cases, the fluorescence signal of the fundus is covered by the fluorescence of the crystalline lens. At a minimum, when FLIO should be applied as a diagnostic tool in elderly populations, technical solutions that avoid the fluorescence of the crystalline lens are necessary.

Using the FLIMX software, the contribution of the separately measured fluorescence of the crystalline lens can be determined in fluorescence measurements of the whole eye. Proposals for the complete elimination of the contribution of the lens fluorescence in fluorescence measurements of the whole eye can be found in the newest patient literature.[245] The attribution of the fluorescence related to single fundus layers might be a goal for future developments. A possible technical solution might be possible by oblique excitation, as published by Zhang et al.[246] Some of the mentioned studies looked only at a small number of patients, such as the studies involving patients with albinism and those with Alzheimer's disease. These studies should be repeated with a larger number of patients.

7 Discussion and Outlook

The investigation of FAF lifetimes *in vivo* presents an innovative way to image the human retina. As this review indicates, there may be many clinical applications in which FLIO can give additional information regarding various retinal diseases. As it is noninvasive and takes only about 2 min, FLIO holds a great potential to emerge into the clinical routine. In the context of a critical analysis, the question of what additional information FLIO may provide needs to be answered, especially with regard to the already established FAF intensity imaging. However, as the name already tells us, FAF intensity imaging accounts only for the intensity of the fluorescence. This technique may hold a lot of potential toward disease diagnosis but within the limit that some fluorophores at the retina make up more of the signal than others. Therefore, subtle changes in fluorophores with minor fluorescence intensity may not be visible in FAF intensity imaging. FLIO on the other hand is independent of the intensity of the fluorescence. Therefore, less intense fluorophores may also impact the measurement. As an example, MP seems to only absorb fluorescence when looking at FAF intensity imaging. Through FLIO, we can observe a direct fluorescence from the retinal carotenoids. This ability of FLIO to observe minor fluorophores may be useful in the imaging of retinal diseases, such as early AMD, MacTel, or Alzheimer's disease. In these diseases, for example, the fundus may appear completely normal on exam, and other conventional imaging such as FAF may also reveal no pathology. Still, FLIO seems to give additional information on subtle changes that start to manifest.

At the current point of research, FLIO is mostly used as a qualitative imaging method, similar to FAF intensity imaging. However, a quantitative approach is possible by investigating the value of individual FAF lifetimes. This is very helpful when quantifying follow-up investigations.

It will be crucial to identify ways to reliably investigate the raw data. New fitting approaches may improve the signal and may reduce the influence of the lens autofluorescence.[245] Another interesting and elegant way to analyze the data is the implication of the "Phasor" approach.[247] Here, the decay data of individual pixels can be distributed in a polar diagram, based on phase and amplitude values, using a Fourier transformation. Individual pixels with similar decays will hereby cluster, possibly allowing individual fluorescent molecules to be distinguished. This approach is available with the latest

software of the SPCImage and has already been used by Dysli et al. in the analysis of FAF lifetimes in GA.[43,53] This approach may hold an alternative opportunity for data analysis and may be useful in the future. Similarly, an automated approach of data analysis would be helpful in a clinical setting.

8 Conclusions

The measurement of FAF lifetimes with the noninvasive Heidelberg Engineering FLIO device may open possibilities for retinal imaging. As shown in multiple studies in clinical settings, FLIO is able to show metabolic alterations that occur in various diseases. FLIO also shows high-contrast, disease-specific patterns. These may lead to a more reliable diagnosis, as has been demonstrated for MacTel. Detecting disease-related patterns in funduscopically healthy eyes may go beyond simple retinal imaging and lead to possibilities for earlier diagnosis. Therefore, FLIO holds a great potential and may eventually find establishment in routine clinical imaging.

Disclosures

No financial disclosures.

Acknowledgments

The authors gratefully thank Heidelberg Engineering for providing the FLIO as well as for their technical assistance. The authors thank Yoshihiko Katayama, PhD, for his technical assistance and Matthias Klemm, PhD, for providing the software FLIMX. The authors also thank the Lowy family and the Lowy Medical Research Institute (LMRI) for their support. Additional support was provided by NIH grants EY11600 and EY14800 and Research to Prevent Blindness. The authors thank all coworkers from the John A. Moran Eye Center and the Sharon Eccles Steele Center for Translational Medicine in Salt Lake City, USA, the University Hospital in Jena, Germany, and the Inselspital in Bern, Switzerland.

References

1. J. Lakowicz, *Principles of Fluorescence Spectroscopy*, Plenum Publishers, New York (1999).
2. C. De Los Santos et al., "FRAP, FLIM, and FRET: detection and analysis of cellular dynamics on a molecular scale using fluorescence microscopy," *Mol. Reprod. Dev.* **82**(7–8), 587–604 (2015).
3. L. C. Chen et al., "Fluorescence lifetime imaging microscopy for quantitative biological imaging," *Methods Cell Biol.* **114**, 457–488 (2013).
4. W. Becker et al., "Fluorescence lifetime imaging by time-correlated single-photon counting," *Microsc. Res. Tech.* **63**(1), 58–66 (2004).
5. B. G. Wang et al., "Intraocular multiphoton microscopy with subcellular spatial resolution by infrared femtosecond lasers," *Histochem. Cell Biol.* **126**(4), 507–515 (2006).
6. M. Han et al., "Age-related structural abnormalities in the human retina-choroid complex revealed by two-photon excited autofluorescence imaging," *J. Biomed. Opt.* **12**(2), 024012 (2007).
7. B. G. Wang et al., "High-resolution two-photon excitation microscopy of ocular tissues in porcine eye," *Lasers Surg. Med.* **40**(4), 247–256 (2008).
8. O. La Schiazza and J. F. Bille, "High-speed two-photon excited autofluorescence imaging of ex vivo human retinal pigment epithelial cells toward age-related macular degeneration diagnostic," *J. Biomed. Opt.* **13**(6), 064008 (2008).
9. S. Peters, M. Hammer, and D. Schweitzer, "Two-photon excited fluorescence microscopy application for ex vivo investigation of ocular fundus samples," *Proc. SPIE* **8086**, 808605 (2011).
10. M. Göppert-Mayer, "Über Elementarakte mit zwei Quantensprüngen," *Ann. Phys.* **401**(3), 273–294 (1931).
11. W. Kaiser and C. G. B. Garrett, "Two-photon excitation in CaF_2: Eu^{2+}," *Phys. Rev. Lett.* **7**(6), 229–231 (1961).
12. W. Denk, J. H. Strickler, and W. W. Webb, "Two-photon laser scanning fluorescence microscopy," *Science* **248**(4951), 73–76 (1990).
13. V. E. Centonze and J. G. White, "Multiphoton excitation provides optical sections from deeper within scattering specimens than confocal imaging," *Biophys. J.* **75**(4), 2015–2024 (1998).
14. A. Periasamy et al., "An evaluation of two-photon excitation versus confocal and digital deconvolution fluorescence microscopy imaging in Xenopus morphogenesis," *Microsc. Res. Tech.* **47**(3), 172–181 (1999).
15. D. Schweitzer et al., "Towards metabolic mapping of the human retina," *Microsc. Res. Tech.* **70**(5), 410–419 (2007).
16. C. Dysli et al., "Fluorescence lifetime imaging ophthalmoscopy," *Prog. Retinal Eye Res.* **60**, 120–143 (2017).
17. K. Suhling, P. M. French, and D. Phillips, "Time-resolved fluorescence microscopy," *Photochem. Photobiol. Sci.* **4**(1), 13–22 (2005).
18. F. C. Delori et al., "In vivo fluorescence of the ocular fundus exhibits retinal pigment epithelium lipofuscin characteristics," *Invest. Ophthalmol. Visual Sci.* **36**(3), 718–729 (1995).
19. D. Schweitzer et al., "Spectral and time-resolved studies on ocular structures," *Proc. SPIE* **6628**, 662807 (2007).
20. M. C. Skala et al., "In vivo multiphoton fluorescence lifetime imaging of protein-bound and free nicotinamide adenine dinucleotide in normal and precancerous epithelia," *J. Biomed. Opt.* **12**(2), 024014 (2007).
21. M. C. Skala et al., "In vivo multiphoton microscopy of NADH and FAD redox states, fluorescence lifetimes, and cellular morphology in precancerous epithelia," *Proc. Natl. Acad. Sci. U. S. A.* **104**(49), 19494–19499 (2007).
22. Y. Imanishi et al., "Noninvasive two-photon imaging reveals retinyl ester storage structures in the eye," *J. Cell Biol.* **164**(3), 373–383 (2004).
23. M. Han et al., "Two-photon excited autofluorescence imaging of human retinal pigment epithelial cells," *J. Biomed. Opt.* **11**(1), 010501 (2006).
24. K. J. Halbhuber and K. Konig, "Modern laser scanning microscopy in biology, biotechnology and medicine," *Ann. Anat.* **185**(1), 1–20 (2003).
25. W. R. Zipfel, R. M. Williams, and W. W. Webb, "Nonlinear magic: multiphoton microscopy in the biosciences," *Nat. Biotechnol.* **21**(11), 1369–1377 (2003).
26. S. Peters et al., "Hydrogen peroxide modulates energy metabolism and oxidative stress in cultures of permanent human Muller cells MIO-M1," *J. Biophotonics* **10**(9), 1180–1188 (2017).
27. M. Griebsch et al., "Hypoxia-induced redox signalling in Muller cells," *Acta Ophthalmol.* **95**(4), e337–e339 (2017).
28. D. Schweitzer et al., "Time-correlated measurement of autofluorescence. A method to detect metabolic changes in the fundus," *Ophthalmologe* **99**(10), 774–779 (2002).
29. A. Neetens and H. Burvenich, "Autofluorescence of optic disc-drusen," *Bull. Soc. Belge Ophtalmol.* **179**, 103–110 (1977).
30. E. Mustonen and H. Nieminen, "Optic disc drusen: a photographic study. I. Autofluorescence pictures and fluorescein angiography," *Acta Ophthalmol.* **60**(6), 849–858 (1982).
31. J. R. Sparrow and M. Boulton, "RPE lipofuscin and its role in retinal pathobiology," *Exp. Eye Res.* **80**(5), 595–606 (2005).
32. S. Dithmar and F. G. Holz, *Fluoreszenzangiographie in der Augenheilkunde: Fluoreszein-Angiographie, Indozyaningrün-Angiographie und Fundus-Autofluoreszenz*, Springer, Berlin (2007).
33. F. G. Holz and R. F. Spaide, *Medical Retina: Focus on Retinal Imaging*, Springer, Heidelberg (2010).
34. A. J. Augustin, *Augenheilkunde*, Springer, Berlin (2007).
35. J. R. Lakowicz, *Principles of Fluorescence Spectroscopy*, Springer, Boston, Massachusetts (2007).
36. L. Marcu, "Fluorescence lifetime techniques in medical applications," *Ann. Biomed. Eng.* **40**(2), 304–331 (2012).
37. D. Schweitzer et al., "Time-resolved autofluorescence imaging of human donor retina tissue from donors with significant extramacular drusen," *Invest. Ophthalmol. Visual Sci.* **53**(7), 3376–3386 (2012).
38. M. Klemm et al., "Repeatability of autofluorescence lifetime imaging at the human fundus in healthy volunteers," *Curr. Eye Res.* **38**(7), 793–801 (2013).

39. D. Schweitzer et al., "In vivo measurement of time-resolved autofluorescence at the human fundus," *J. Biomed. Opt.* **9**(6), 1214–1222 (2004).
40. C. Dysli et al., "Quantitative analysis of fluorescence lifetime measurements of the macula using the fluorescence lifetime imaging ophthalmoscope in healthy subjects," *Invest. Ophthalmol. Visual Sci.* **55**(4), 2106–2113 (2014).
41. C. Dysli, S. Wolf, and M. S. Zinkernagel, "Fluorescence lifetime imaging in retinal artery occlusion," *Invest. Ophthalmol. Visual Sci.* **56**(5), 3329–3336 (2015).
42. C. Dysli et al., "Fluorescence lifetime imaging in Stargardt disease: potential marker for disease progression," *Invest. Ophthalmol. Visual Sci.* **57**(3), 832–841 (2016).
43. C. Dysli, S. Wolf, and M. S. Zinkernagel, "Autofluorescence lifetimes in geographic atrophy in patients with age-related macular degeneration," *Invest. Ophthalmol. Visual Sci.* **57**(6), 2479–2487 (2016).
44. C. Dysli et al., "Fluorescence lifetimes of drusen in age-related macular degeneration," *Invest. Ophthalmol. Visual Sci.* **58**(11), 4856–4862 (2017).
45. L. Sauer et al., "Impact of macular pigment on fundus autofluorescence lifetimes," *Invest. Ophthalmol. Visual Sci.* **56**(8), 4668–4679 (2015).
46. L. Sauer et al., "Monitoring macular pigment changes in macular holes using fluorescence lifetime imaging ophthalmoscopy," *Acta Ophthalmol.* **95**(5), 481–492 (2017).
47. J. Schmidt et al., "Fundus autofluorescence lifetimes are increased in non-proliferative diabetic retinopathy," *Acta Ophthalmol.* **95**(1), 33–40 (2017).
48. L. Sauer et al., "Fluorescence lifetime imaging ophthalmoscopy (FLIO): a novel way to assess macular telangiectasia type 2 (MacTel)," *Ophthalmol. Retina* **2**, 587–598 (2018).
49. C. Dysli et al., "Fundus autofluorescence lifetimes and central serous chorioretinopathy," *Retina* **37**(11), 2151–2161 (2017).
50. L. Sauer et al., "Monitoring foveal sparing in geographic atrophy with fluorescence lifetime imaging ophthalmoscopy: a novel approach," *Acta Ophthalmol.* **96**(3), 257–266 (2018).
51. S. Jentsch et al., "Retinal fluorescence lifetime imaging ophthalmoscopy measures depend on the severity of Alzheimer's disease," *Acta Ophthalmol.* **93**, e241–e247 (2015).
52. M. Klemm et al., "FLIMX: a software package to determine and analyze the fluorescence lifetime in time-resolved fluorescence data from the human eye," *PloS One* **10**(7), e0131640 (2015).
53. W. Becker, *The bh TCSPC Handbook*, 6th ed., Becker and Hickl GmbH, Berlin (2014).
54. D. Schweitzer, "Autofluorescence diagnostics of ophthalmic diseases," in *Natural Biomarkers for Cellular Metabolism—Biology, Techniques, and Applications*, V. V. Ghukasyan and A. A. Heikal, Eds., pp. 317–344, Taylor and Francis Group, CRC Press (2014).
55. M. L. Katz et al., "Influence of early photoreceptor degeneration on lipofuscin in the retinal pigment epithelium," *Exp. Eye Res.* **43**(4), 561–573 (1986).
56. F. C. Delori, D. G. Goger, and C. K. Dorey, "Age-related accumulation and spatial distribution of lipofuscin in RPE of normal subjects," *Invest. Ophthalmol. Visual Sci.* **42**(8), 1855–1866 (2001).
57. G. E. Eldred and M. L. Katz, "Fluorophores of the human retinal pigment epithelium: separation and spectral characterization," *Exp. Eye Res.* **47**(1), 71–86 (1988).
58. P. K. Chowdhury et al., "Generation of fluorescent adducts of malondialdehyde and amino acids: toward an understanding of lipofuscin," *Photochem. Photobiol.* **79**(1), 21–25 (2004).
59. J. R. Sparrow et al., "The bisretinoids of retinal pigment epithelium," *Prog. Retinal Eye Res.* **31**(2), 121–135 (2012).
60. R. S. Sohal, "Assay of lipofuscin/ceroid pigment in vivo during aging," *Methods Enzymol.* **105**, 484–487 (1984).
61. F. G. Holz et al., "Inhibition of lysosomal degradative functions in RPE cells by a retinoid component of lipofuscin," *Invest. Ophthalmol. Visual Sci.* **40**(3), 737–743 (1999).
62. F. G. Holz et al., "Fundus autofluorescence and development of geographic atrophy in age-related macular degeneration," *Invest. Ophthalmol. Visual Sci.* **42**(5), 1051–1056 (2001).
63. L. S. Murdaugh et al., "Compositional studies of human RPE lipofuscin," *J. Mass Spectrom.* **45**(10), 1139–1147 (2010).
64. Z. Ablonczy et al., "Lack of correlation between the spatial distribution of A2E and lipofuscin fluorescence in the human retinal pigment epithelium," *Invest. Ophthalmol. Visual Sci.* **54**(8), 5535–5542 (2013).
65. R. T. Smith, P. S. Bernstein, and C. A. Curcio, "Rethinking A2E," *Invest. Ophthalmol. Visual Sci.* **54**(8), 5543 (2013).
66. R. A. Bone, J. T. Landrum, and S. L. Tarsis, "Preliminary identification of the human macular pigment," *Vision Res.* **25**(11), 1531–1535 (1985).
67. R. A. Bone et al., "Stereochemistry of the human macular carotenoids," *Invest. Ophthalmol. Visual Sci.* **34**(6), 2033–2040 (1993).
68. D. M. Snodderly, J. D. Auran, and F. C. Delori, "The macular pigment. II. Spatial distribution in primate retinas," *Invest. Ophthalmol. Visual Sci.* **25**(6), 674–685 (1984).
69. A. Kijlstra et al., "Lutein: more than just a filter for blue light," *Prog. Retinal Eye Res.* **31**(4), 303–315 (2012).
70. M. Sharifzadeh, P. S. Bernstein, and W. Gellermann, "Nonmydriatic fluorescence-based quantitative imaging of human macular pigment distributions," *J. Opt. Soc. Am. A* **23**(10), 2373–2387 (2006).
71. P. Bhosale and P. S. Bernstein, "Vertebrate and invertebrate carotenoid-binding proteins," *Arch. Biochem. Biophys.* **458**(2), 121–127 (2007).
72. E. Loane et al., "Transport and retinal capture of lutein and zeaxanthin with reference to age-related macular degeneration," *Surv. Ophthalmol.* **53**(1), 68–81 (2008).
73. P. Bhosale et al., "Identification and characterization of a Pi isoform of glutathione S-transferase (GSTP1) as a zeaxanthin-binding protein in the macula of the human eye," *J. Biol. Chem.* **279**(47), 49447–49454 (2004).
74. P. Bhosale and P. S. Bernstein, "Synergistic effects of zeaxanthin and its binding protein in the prevention of lipid membrane oxidation," *Biochim. Biophys. Acta* **1740**(2), 116–121 (2005).
75. P. Bhosale et al., "Purification and partial characterization of a lutein-binding protein from human retina," *Biochemistry* **48**(22), 4798–4807 (2009).
76. P. S. Bernstein et al., "Retinal tubulin binds macular carotenoids," *Invest. Ophthalmol. Visual Sci.* **38**(1), 167–175 (1997).
77. P. S. Bernstein et al., "Lutein, zeaxanthin, and meso-zeaxanthin: the basic and clinical science underlying carotenoid-based nutritional interventions against ocular disease," *Prog. Retinal Eye Res.* **50**, 34–66 (2016).
78. A. A. Woodall, G. Britton, and M. J. Jackson, "Carotenoids and protection of phospholipids in solution or in liposomes against oxidation by peroxyl radicals: relationship between carotenoid structure and protective ability," *Biochim. Biophys. Acta.* **1336**(3), 575–586 (1997).
79. W. T. Ham, Jr. et al., "Histologic analysis of photochemical lesions produced in rhesus retina by short-wave-length light," *Invest. Ophthalmol. Visual Sci.* **17**(10), 1029–1035 (1978).
80. N. I. Krinsky, "Antioxidant functions of carotenoids," *Free Radical Biol. Med.* **7**(6), 617–635 (1989).
81. R. A. Bone et al., "Distribution of lutein and zeaxanthin stereoisomers in the human retina," *Exp. Eye Res.* **64**(2), 211–218 (1997).
82. I. V. Ermakov et al., "Resonant Raman detection of macular pigment levels in the living human retina," *Opt. Lett.* **26**(4), 202–204 (2001).
83. I. V. Ermakov, M. R. Ermakova, and W. Gellermann, "Simple Raman instrument for in vivo detection of macular pigments," *Appl. Spectrosc.* **59**(7), 861–867 (2005).
84. J. R. Lakowicz et al., "Fluorescence lifetime imaging of free and protein-bound NADH," *Proc. Natl. Acad. Sci. U. S. A.* **89**(4), 1271–1275 (1992).
85. K. Koenig and H. Schneckenburger, "Laser-induced autofluorescence for medical diagnosis," *J. Fluoresc.* **4**(1), 17–40 (1994).
86. D. Chorvat and A. Chorvatova, "Multi-wavelength fluorescence lifetime spectroscopy: a new approach to the study of endogenous fluorescence in living cells and tissues," *Laser Phys. Lett.* **6**(3), 175–193 (2009).
87. B. Chance, "Pyridine nucleotide as an indicator of the oxygen requirements for energy-linked functions of mitochondria," *Circ. Res.* **38**(5 Suppl. 1), I31–38 (1976).
88. M. Wakita, G. Nishimura, and M. Tamura, "Some characteristics of the fluorescence lifetime of reduced pyridine nucleotides in isolated mitochondria, isolated hepatocytes, and perfused rat liver in situ," *J. Biochem.* **118**(6), 1151–1160 (1995).
89. R. Niesner et al., "Noniterative biexponential fluorescence lifetime imaging in the investigation of cellular metabolism by means of NAD(P)H autofluorescence," *ChemPhysChem* **5**(8), 1141–1149 (2004).

90. H. Schneckenburger et al., "Autofluorescence lifetime imaging of cultivated cells using a UV picosecond laser diode," *J. Fluoresc.* **14**(5), 649–654 (2004).
91. B. Kierdaszuk et al., "Fluorescence of reduced nicotinamides using one- and two-photon excitation," *Biophys. Chem.* **62**(1–3), 1–13 (1996).
92. T. Ihanamaki, L. J. Pelliniemi, and E. Vuorio, "Collagens and collagen-related matrix components in the human and mouse eye," *Prog. Retinal Eye Res.* **23**(4), 403–434 (2004).
93. J. Blomfield and J. F. Farrar, "The fluorescent properties of maturing arterial elastin," *Cardiovasc. Res.* **3**(2), 161–170 (1969).
94. D. Fujimoto and T. Moriguchi, "Pyridinoline, a non-reducible cross-link of collagen. Quantitative determination, distribution, and isolation of a crosslinked peptide," *J. Biochem.* **83**(3), 863–867 (1978).
95. R. Richards-Kortum and E. Sevick-Muraca, "Quantitative optical spectroscopy for tissue diagnosis," *Annu. Rev. Phys. Chem.* **47**, 555–606 (1996).
96. J. H. Aiken and C. W. Huie, "Detection of bilirubin using surfactant fluorescence enhancement and visible laser fluorometry," *Anal. Lett.* **24**(1), 167–180 (1991).
97. A. H. Colbert and A. A. Heikal, "Towards probing skin cancer using endogenous melanin fluorescence," *The Penn State McNair J.* 8 (2005).
98. F. N. Ghadially, W. J. Neish, and H. C. Dawkins, "Mechanisms involved in the production of red fluorescence of human and experimental tumours," *J. Pathol. Bacteriol.* **85**, 77–92 (1963).
99. R. Cubeddu et al., "Fluorescence lifetime imaging: an application to the detection of skin tumors," *IEEE J. Sel. Top. Quantum Electron.* **5**(4), 923–929 (1999).
100. W. G. John and E. J. Lamb, "The Maillard or browning reaction in diabetes," *Eye* **7**(Pt. 2), 230–237 (1993).
101. D. Schweitzer, "Metabolic mapping," in *Medical Retina*, F. Holz and R. Spaide, Eds., pp. 107–123, Springer, Berlin, Heidelberg (2010).
102. L. Sauer et al., "Fluorescence lifetime imaging ophthalmoscopy (FLIO) of macular pigment," *Invest. Ophthalmol. Visual Sci.* **59**(7), 3094–3103 (2018).
103. P. S. Harvey, R. A. King, and C. G. Summers, "Spectrum of foveal development in albinism detected with optical coherence tomography," *J. AAPOS* **10**(3), 237–242 (2006).
104. Z. Gregor, "The perifoveal vasculature in albinism," *Br. J. Ophthalmol.* **62**(8), 554–557 (1978).
105. R. V. Abadi and M. J. Cox, "The distribution of macular pigment in human albinos," *Invest. Ophthalmol. Visual Sci.* **33**(3), 494–497 (1992).
106. J. R. Sparrow, D. Hicks, and C. P. Hamel, "The retinal pigment epithelium in health and disease," *Curr. Mol. Med.* **10**(9), 802–823 (2010).
107. Y. Wolfson et al., "Evidence of macular pigment in the central macula in albinism," *Exp. Eye Res.* **145**, 468–471 (2016).
108. C. M. Putnam and P. J. Bland, "Macular pigment optical density spatial distribution measured in a subject with oculocutaneous albinism," *J. Optom.* **7**(4), 241–245 (2014).
109. R. Klein et al., "The prevalence of age-related macular degeneration and associated risk factors," *Arch Ophthalmol.* **128**(6), 750–758 (2010).
110. D. S. Friedman et al., "Prevalence of age-related macular degeneration in the United States," *Arch Ophthalmol.* **122**(4), 564–572 (2004).
111. K. M. Gehrs et al., "Age-related macular degeneration: emerging pathogenetic and therapeutic concepts," *Ann. Med.* **38**(7), 450–471 (2006).
112. J. M. Seddon, U. A. Ajani, and B. D. Mitchell, "Familial aggregation of age-related maculopathy," *Am. J. Ophthalmol.* **123**(2), 199–206 (1997).
113. C. J. Hammond et al., "Genetic influence on early age-related maculopathy: a twin study," *Ophthalmology* **109**(4), 730–736 (2002).
114. S. M. Meyers, T. Greene, and F. A. Gutman, "A twin study of age-related macular degeneration," *Am. J. Ophthalmol.* **120**(6), 757–766 (1995).
115. I. Taskintuna, M. E. Elsayed, and P. Schatz, "Update on clinical trials in dry age-related macular degeneration," *Middle East Afr. J. Ophthalmol.* **23**(1), 13–26 (2016).
116. S. Beatty et al., "Macular pigment and risk for age-related macular degeneration in subjects from a Northern European population," *Invest. Ophthalmol. Visual Sci.* **42**(2), 439–446 (2001).
117. R. A. Bone et al., "Macular pigment in donor eyes with and without AMD: a case-control study," *Invest. Ophthalmol. Visual Sci.* **42**(1), 235–240 (2001).
118. J. M. Nolan et al., "Risk factors for age-related maculopathy are associated with a relative lack of macular pigment," *Exp. Eye Res.* **84**(1), 61–74 (2007).
119. K. O. Akuffo et al., "Relationship between macular pigment and visual function in subjects with early age-related macular degeneration," *Br. J. Ophthalmol.* **101**(2), 190–197 (2017).
120. D. M. Snodderly, "Evidence for protection against age-related macular degeneration by carotenoids and antioxidant vitamins," *Am. J. Clin. Nutr.* **62**(Suppl. 6), 1448S–1461S (1995).
121. P. Bhosale, B. Serban, and P. S. Bernstein, "Retinal carotenoids can attenuate formation of A2E in the retinal pigment epithelium," *Arch. Biochem. Biophys.* **483**(2), 175–181 (2009).
122. Age-Related Eye Disease Study 2 Research Group, "Lutein + zeaxanthin and omega-3 fatty acids for age-related macular degeneration: the age-related eye disease study 2 (AREDS2) randomized clinical trial," *JAMA* **309**(19), 2005–2015 (2013).
123. W. Andreatta and S. El-Sherbiny, "Evidence-based nutritional advice for patients affected by age-related macular degeneration," *Ophthalmologica* **231**(4), 185–190 (2014).
124. M. D. Pinazo-Duran et al., "Do nutritional supplements have a role in age macular degeneration prevention?" *J. Ophthalmol.* **2014**, 1–15 (2014).
125. Age-Related Eye Disease Study 2 Research Group et al., "Secondary analyses of the effects of lutein/zeaxanthin on age-related macular degeneration progression: AREDS2 report No. 3," *JAMA Ophthalmol.* **132**(2), 142–149 (2014).
126. A. Gorusupudi, K. Nelson, and P. S. Bernstein, "The age-related eye disease 2 study: micronutrients in the treatment of macular degeneration," *Adv. Nutr.* **8**(1), 40–53 (2017).
127. S. Beatty, F. J. van Kuijk, and U. Chakravarthy, "Macular pigment and age-related macular degeneration: longitudinal data and better techniques of measurement are needed," *Invest. Ophthalmol. Visual Sci.* **49**(3), 843–845 (2008).
128. Age-Related Eye Disease Study Research Group, "A randomized, placebo-controlled, clinical trial of high-dose supplementation with vitamins C and E, beta carotene, and zinc for age-related macular degeneration and vision loss: AREDS report no. 8," *Arch Ophthalmol.* **119**(10), 1417–1436 (2001).
129. M. R. Munk et al., "Macular atrophy in patients with long-term anti-VEGF treatment for neovascular age-related macular degeneration," *Acta Ophthalmol.* **94**(8), e757–e764 (2016).
130. F. G. Holz et al., "Geographic atrophy: clinical features and potential therapeutic approaches," *Ophthalmology* **121**(5), 1079–1091 (2014).
131. A. Bindewald et al., "Classification of fundus autofluorescence patterns in early age-related macular disease," *Invest. Ophthalmol. Visual Sci.* **46**(9), 3309–3314 (2005).
132. S. Schmitz-Valckenberg et al., "Correlation between the area of increased autofluorescence surrounding geographic atrophy and disease progression in patients with AMD," *Invest. Ophthalmol. Visual Sci.* **47**(6), 2648–2654 (2006).
133. R. T. Smith et al., "Autofluorescence characteristics of early, atrophic, and high-risk fellow eyes in age-related macular degeneration," *Invest. Ophthalmol. Visual Sci.* **47**(12), 5495–5504 (2006).
134. M. Gliem et al., "Quantitative fundus autofluorescence in early and intermediate age-related macular degeneration," *JAMA Ophthalmol.* **134**(7), 817–824 (2016).
135. D. Schweitzer et al., "Comparison of parameters of time-resolved autofluorescence between healthy subjects and patients suffering from early AMD," *Ophthalmologe* **106**(8), 714–722 (2009).
136. L. Sauer et al., "Patterns of fundus autofluorescence lifetimes in eyes of individuals with non-exudative age-related macular degeneration," *Invest. Ophthalmol. Visual Sci.* **59**(4), AMD65–AMD77 (2018).
137. K. N. Khan et al., "Differentiating drusen: drusen and drusen-like appearances associated with ageing, age-related macular degeneration, inherited eye disease and other pathological processes," *Prog. Retinal Eye Res.* **53**, 70–106 (2016).
138. F. Donders, "Beiträge zur pathologischen Anatomie des Auges," *Graefe's Arch. Clin. Exp. Ophthalmol.* **2**, 106–118 (1855).

139. G. S. Hageman and R. F. Mullins, "Molecular composition of drusen as related to substructural phenotype," *Mol. Vis.* **5**, 28 (1999).
140. G. S. Hageman et al., "An integrated hypothesis that considers drusen as biomarkers of immune-mediated processes at the RPE-Bruch's membrane interface in aging and age-related macular degeneration," *Prog. Retinal Eye Res.* **20**(6), 705–732 (2001).
141. D. H. Anderson et al., "The pivotal role of the complement system in aging and age-related macular degeneration: hypothesis re-visited," *Prog. Retinal Eye Res.* **29**(2), 95–112 (2010).
142. D. H. Anderson et al., "A role for local inflammation in the formation of drusen in the aging eye," *Am. J. Ophthalmol.* **134**(3), 411–431 (2002).
143. F. L. Ferris, 3rd et al., "Clinical classification of age-related macular degeneration," *Ophthalmology* **120**(4), 844–851 (2013).
144. J. S. Sunness, "The natural history of geographic atrophy, the advanced atrophic form of age-related macular degeneration," *Mol. Vis.* **5**, 24–35 (1999).
145. S. H. Sarks, "Drusen patterns predisposing to geographic atrophy of the retinal pigment epithelium," *Aust. J. Ophthalmol.* **10**(2), 91–97 (1982).
146. J. P. Sarks, S. H. Sarks, and M. C. Killingsworth, "Evolution of geographic atrophy of the retinal pigment epithelium," *Eye* **2**(Pt. 5), 552–577 (1988).
147. P. Maguire and A. K. Vine, "Geographic atrophy of the retinal pigment epithelium," *Am. J. Ophthalmol.* **102**(5), 621–625 (1986).
148. H. Schatz and H. R. McDonald, "Atrophic macular degeneration. Rate of spread of geographic atrophy and visual loss," *Ophthalmology* **96**(10), 1541–1551 (1989).
149. M. Yung, M. A. Klufas, and D. Sarraf, "Clinical applications of fundus autofluorescence in retinal disease," *Int. J. Retina Vitreous* **2**, 12 (2016).
150. D. G. Cogan and T. Kuwabara, "Capillary shunts in the pathogenesis of diabetic retinopathy," *Diabetes* **12**, 293–300 (1963).
151. X. Y. Zhang et al., "Diabetic macular edema: new concepts in pathophysiology and treatment," *Cell Biosci.* **4**, 27 (2014).
152. A. J. Barber, T. W. Gardner, and S. F. Abcouwer, "The significance of vascular and neural apoptosis to the pathology of diabetic retinopathy," *Invest. Ophthalmol. Visual Sci.* **52**(2), 1156–1163 (2011).
153. D. Y. Yu et al., "Pathogenesis and intervention strategies in diabetic retinopathy," *Clin. Exp. Ophthalmol.* **29**(3), 164–166 (2001).
154. M. P. de la Maza et al., "Fluorescent advanced glycation end-products (ages) detected by spectro-photofluorimetry, as a screening tool to detect diabetic microvascular complications," *J. Diabetes Mellitus* **2**(2), 221–226 (2012).
155. S. Vujosevic et al., "Diabetic macular edema: fundus autofluorescence and functional correlations," *Invest. Ophthalmol. Visual Sci.* **52**(1), 442–448 (2011).
156. M. Hammer et al., "Ocular fundus auto-fluorescence observations at different wavelengths in patients with age-related macular degeneration and diabetic retinopathy," *Graefe's Arch. Clin. Exp. Ophthalmol.* **246**(1), 105–114 (2008).
157. D. Schweitzer et al., "Fluorescence lifetime imaging ophthalmoscopy in type 2 diabetic patients who have no signs of diabetic retinopathy," *J. Biomed. Opt.* **20**(6), 061106 (2015).
158. P. C. Issa et al., "Macular telangiectasia type 2," *Prog. Retinal Eye Res.* **34**, 49–77 (2013).
159. P. C. Issa, F. G. Holz, and H. P. Scholl, "Metamorphopsia in patients with macular telangiectasia type 2," *Doc. Ophthalmol.* **119**(2), 133–140 (2009).
160. R. P. Finger et al., "Reading performance is reduced by parafoveal scotomas in patients with macular telangiectasia type 2," *Invest. Ophthalmol. Visual Sci.* **50**(3), 1366–1370 (2009).
161. T. E. Clemons et al., "The national eye institute visual function questionnaire in the macular telangiectasia (MacTel) project," *Invest. Ophthalmol. Visual Sci.* **49**(10), 4340–4346 (2008).
162. T. E. Clemons et al., "Baseline characteristics of participants in the natural history study of macular telangiectasia (MacTel) MacTel project report no. 2," *Ophthalmic Epidemiol.* **17**(1), 66–73 (2010).
163. T. F. Heeren et al., "Progression of vision loss in macular telangiectasia type 2," *Invest. Ophthalmol. Visual Sci.* **56**(6), 3905–3912 (2015).
164. N. L. Parmalee et al., "Analysis of candidate genes for macular telangiectasia type 2," *Mol. Vis.* **16**, 2718–2726 (2010).
165. N. L. Parmalee et al., "Identification of a potential susceptibility locus for macular telangiectasia type 2," *PloS One* **7**(8), e24268 (2012).
166. M. C. Gillies et al., "Familial asymptomatic macular telangiectasia type 2," *Ophthalmology* **116**(12), 2422–2429 (2009).
167. L. Delaere, L. Spielberg, and A. M. Leys, "Vertical transmission of macular telangiectasia type 2," *Retinal Cases Brief Rep.* **6**(3), 253–257 (2012).
168. T. S. Scerri et al., "Genome-wide analyses identify common variants associated with macular telangiectasia type 2," *Nat. Genet.* **49**(4), 559–567 (2017).
169. H. M. Helb et al., "Abnormal macular pigment distribution in type 2 idiopathic macular telangiectasia," *Retina* **28**(6), 808–816 (2008).
170. M. B. Zeimer et al., "Idiopathic macular telangiectasia type 2: distribution of macular pigment and functional investigations," *Retina* **30**(4), 586–595 (2010).
171. F. C. Delori et al., "Macular pigment density measured by autofluorescence spectrometry: comparison with reflectometry and heterochromatic flicker photometry," *J. Opt. Soc. Am. A* **18**(6), 1212–1230 (2001).
172. S. D. Esposti et al., "Macular pigment parameters in patients with macular telangiectasia (MacTel) and normal subjects: implications of a novel analysis," *Invest. Ophthalmol. Visual Sci.* **53**(10), 6568–6575 (2012).
173. R. Y. Choi et al., "Macular pigment distribution responses to high-dose zeaxanthin supplementation in patients with macular telangiectasia type 2," *Retina* **37**(12), 2238–2247 (2017).
174. E. K. Chin et al., "Staging of macular telangiectasia: power-Doppler optical coherence tomography and macular pigment optical density," *Invest. Ophthalmol. Visual Sci.* **54**(7), 4459–4470 (2013).
175. B. Li et al., "Retinal accumulation of zeaxanthin, lutein, and beta-carotene in mice deficient in carotenoid cleavage enzymes," *Exp. Eye Res.* **159**, 123–131 (2017).
176. J. L. Kovach and P. J. Rosenfeld, "Bevacizumab (avastin) therapy for idiopathic macular telangiectasia type II," *Retina* **29**(1), 27–32 (2009).
177. A. B. Roller et al., "Intravitreal bevacizumab for treatment of proliferative and nonproliferative type 2 idiopathic macular telangiectasia," *Retina* **31**(9), 1848–1855 (2011).
178. H. Mehta et al., "Natural history and effect of therapeutic interventions on subretinal fluid causing foveal detachment in macular telangiectasia type 2," *Br. J. Ophthalmol.* **101**(7), 955–959 (2017).
179. F. Bucher et al., "CNTF attenuates vasoproliferative changes through upregulation of SOCS3 in a mouse-model of oxygen-induced retinopathy," *Invest. Ophthalmol. Visual Sci.* **57**(10), 4017–4026 (2016).
180. R. Klein et al., "The prevalence of macular telangiectasia type 2 in the Beaver Dam eye study," *Am. J. Ophthalmol.* **150**(1), 55–62.e2 (2010).
181. F. B. Sallo et al., "The prevalence of type 2 idiopathic macular telangiectasia in two African populations," *Ophthalmic Epidemiol.* **19**(4), 185–189 (2012).
182. F. B. Sallo et al., "Multimodal imaging in type 2 idiopathic macular telangiectasia," *Retina* **35**(4), 742–749 (2015).
183. L. Toto et al., "Multimodal imaging of macular telangiectasia type 2: focus on vascular changes using optical coherence tomography angiography," *Invest. Ophthalmol. Visual Sci.* **57**(9), OCT268–OCT276 (2016).
184. W. T. Wong et al., "Fundus autofluorescence in type 2 idiopathic macular telangiectasia: correlation with optical coherence tomography and microperimetry," *Am. J. Ophthalmol.* **148**(4), 573–583 (2009).
185. M. Niskopoulou et al., "Is indocyanine green angiography useful for the diagnosis of macular telangiectasia type 2?" *Br. J. Ophthalmol.* **97**(7), 946–948 (2013).
186. F. B. Sallo et al., "'En face' OCT imaging of the IS/OS junction line in type 2 idiopathic macular telangiectasia," *Invest. Ophthalmol. Visual Sci.* **53**(10), 6145–6152 (2012).
187. L. Wu, T. Evans, and J. F. Arevalo, "Idiopathic macular telangiectasia type 2 (idiopathic juxtafoveolar retinal telangiectasis type 2A, Mac Tel 2)," *Surv. Ophthalmol.* **58**(6), 536–559 (2013).
188. V. Surguch, M. A. Gamulescu, and V. P. Gabel, "Optical coherence tomography findings in idiopathic juxtafoveal retinal telangiectasis," *Graefe's Arch. Clin. Exp. Ophthalmol.* **245**(6), 783–788 (2007).
189. W. H. Stern and D. B. Archer, "Retinal vascular occlusion," *Annu. Rev. Med.* **32**, 101–106 (1981).

190. S. S. Hayreh, "Ocular vascular occlusive disorders: natural history of visual outcome," *Prog. Retinal Eye Res.* **41**, 1–25 (2014).
191. S. J. Ahn et al., "Retinal and choroidal changes and visual outcome in central retinal artery occlusion: an optical coherence tomography study," *Am. J. Ophthalmol.* **159**(4), 667–676.e1 (2015).
192. O. Furashova and E. Matthe, "Retinal changes in different grades of retinal artery occlusion: an optical coherence tomography study," *Invest. Ophthalmol. Visual Sci.* **58**(12), 5209–5216 (2017).
193. D. Schweitzer et al., "Time-resolved autofluorescence in retinal vascular occlusions," *Ophthalmologe* **107**(12), 1145–1152 (2010).
194. C. Bonne, A. Muller, and M. Villain, "Free radicals in retinal ischemia," *Gen. Pharmacol.* **30**(3), 275–280 (1998).
195. H. Kuriyama et al., "Involvement of oxygen free radicals in experimental retinal ischemia and the selective vulnerability of retinal damage," *Ophthalmic Res.* **33**(4), 196–202 (2001).
196. A. Siskova and J. Wilhelm, "The effects of hyperoxia, hypoxia, and ischemia/reperfusion on the activity of cytochrome oxidase from the rat retina," *Physiol. Res.* **50**(3), 267–273 (2001).
197. W. Xu et al., "Increased oxidative stress is associated with chronic intermittent hypoxia-mediated brain cortical neuronal cell apoptosis in a mouse model of sleep APNEA," *Neuroscience* **126**(2), 313–323 (2004).
198. A. A. Heikal, "Intracellular coenzymes as natural biomarkers for metabolic activities and mitochondrial anomalies," *Biomark Med.* **4**(2), 241–263 (2010).
199. R. Mathew, E. Papavasileiou, and S. Sivaprasad, "Autofluorescence and high-definition optical coherence tomography of retinal artery occlusions," *Clin. Ophthalmol.* **4**, 1159–1163 (2010).
200. M. Michaelides, D. M. Hunt, and A. T. Moore, "The genetics of inherited macular dystrophies," *J. Med. Genet.* **40**(9), 641–650 (2003).
201. E. M. Stone et al., "Clinically focused molecular investigation of 1000 consecutive families with inherited retinal disease," *Ophthalmology* **124**(9), 1314–1331 (2017).
202. R. Allikmets et al., "A photoreceptor cell-specific ATP-binding transporter gene (ABCR) is mutated in recessive stargardt macular dystrophy," *Nat. Genet.* **15**(3), 236–246 (1997).
203. R. A. Lewis et al., "Genotype/phenotype analysis of a photoreceptor-specific ATP-binding cassette transporter gene, ABCR, in stargardt disease," *Am. J. Hum. Genet.* **64**(2), 422–434 (1999).
204. N. P. Boyer et al., "Lipofuscin and N-retinylidene-N-retinylethanolamine (A2E) accumulate in retinal pigment epithelium in absence of light exposure: their origin is 11-cis-retinal," *J. Biol. Chem.* **287**(26), 22276–22286 (2012).
205. N. Zhang et al., "Protein misfolding and the pathogenesis of ABCA4-associated retinal degenerations," *Hum. Mol. Genet.* **24**(11), 3220–3237 (2015).
206. A. V. Cideciyan et al., "Mutations in ABCA4 result in accumulation of lipofuscin before slowing of the retinoid cycle: a reappraisal of the human disease sequence," *Hum. Mol. Genet.* **13**(5), 525–534 (2004).
207. Y. Chen et al., "Mechanism of all-trans-retinal toxicity with implications for stargardt disease and age-related macular degeneration," *J. Biol. Chem.* **287**(7), 5059–5069 (2012).
208. T. R. Burke et al., "Quantitative fundus autofluorescence in recessive stargardt disease," *Invest. Ophthalmol. Visual Sci.* **55**(5), 2841–2852 (2014).
209. V. A. McBain, J. Townend, and N. Lois, "Progression of retinal pigment epithelial atrophy in stargardt disease," *Am. J. Ophthalmol.* **154**(1), 146–154 (2012).
210. Z. Ablonczy et al., "Molecule-specific imaging and quantitation of A2E in the RPE," *Adv. Exp. Med. Biol.* **723**, 75–81 (2012).
211. A. E. Sears et al., "Towards treatment of stargardt disease: workshop organized and sponsored by the foundation fighting blindness," *Transl. Vision Sci. Technol.* **6**(5), 6 (2017).
212. P. C. Issa et al., "Fundus autofluorescence in the Abca4$^{-/-}$ mouse model of stargardt disease—correlation with accumulation of A2E, retinal function, and histology," *Invest. Ophthalmol. Visual Sci.* **54**(8), 5602–5612 (2013).
213. J. R. Sparrow et al., "Flecks in recessive stargardt disease: short-wavelength autofluorescence, near-infrared autofluorescence, and optical coherence tomography," *Invest. Ophthalmol. Visual Sci.* **56**(8), 5029–5039 (2015).
214. P. Iacono et al., "Central serous chorioretinopathy treatments: a mini review," *Ophthalmic Res.* **55**(2), 76–83 (2015).
215. R. H. Loo et al., "Factors associated with reduced visual acuity during long-term follow-up of patients with idiopathic central serous chorioretinopathy," *Retina* **22**(1), 19–24 (2002).
216. C. M. Gilbert et al., "Long-term follow-up of central serous chorioretinopathy," *Br. J. Ophthalmol.* **68**(11), 815–820 (1984).
217. B. Nicholson et al., "Central serous chorioretinopathy: update on pathophysiology and treatment," *Surv. Ophthalmol.* **58**(2), 103–126 (2013).
218. B. Liu, T. Deng, and J. Zhang, "Risk factors for central serous chorioretinopathy: a systematic review and meta-analysis," *Retina* **36**(1), 9–19 (2016).
219. A. Daruich et al., "Central serous chorioretinopathy: recent findings and new physiopathology hypothesis," *Prog. Retinal Eye Res.* **48**, 82–118 (2015).
220. H. Matsumoto et al., "Fundus autofluorescence of elongated photoreceptor outer segments in central serous chorioretinopathy," *Am. J. Ophthalmol.* **151**(4), 617–623.e1, e611 (2011).
221. M. S. Zinkernagel and R. E. MacLaren, "Recent advances and future prospects in choroideremia," *Clin. Ophthalmol.* **9**, 2195–2200 (2015).
222. R. E. MacLaren et al., "Retinal gene therapy in patients with choroideremia: initial findings from a phase 1/2 clinical trial," *Lancet* **383**(9923), 1129–1137 (2014).
223. J. K. Jolly et al., "A qualitative and quantitative assessment of fundus autofluorescence patterns in patients with choroideremia," *Invest. Ophthalmol. Visual Sci.* **57**(10), 4498–4503 (2016).
224. C. Dysli et al., "Autofluorescence lifetimes in patients with choroideremia identify photoreceptors in areas with retinal pigment epithelium atrophy," *Invest. Ophthalmol. Visual Sci.* **57**(15), 6714–6721 (2016).
225. A. F. Goldberg, O. L. Moritz, and D. S. Williams, "Molecular basis for photoreceptor outer segment architecture," *Prog. Retinal Eye Res.* **55**, 52–81 (2016).
226. D. T. Hartong, E. L. Berson, and T. P. Dryja, "Retinitis pigmentosa," *Lancet* **368**(9549), 1795–1809 (2006).
227. S. Shankar, "Hereditary retinal and choroidal dystrophies," in *Emery and Rimoin's Principles and Practice of Medical Genetics*, D. Rimoin, R. Pyeritz, and B. Korf, Eds., pp. 1–18, Academic Press (2013).
228. S. Ferrari et al., "Retinitis pigmentosa: genes and disease mechanisms," *Curr. Genomics* **12**(4), 238–249 (2011).
229. Q. Zhang, "Retinitis pigmentosa: progress and perspective," *Asia Pac. J. Ophthalmol.* **5**(4), 265–271 (2016).
230. S. P. Daiger, S. J. Bowne, and L. S. Sullivan, "Perspective on genes and mutations causing retinitis pigmentosa," *Arch Ophthalmol.* **125**(2), 151–158 (2007).
231. G. A. Fishman, "Retinitis pigmentosa: visual loss," *Arch Ophthalmol.* **96**(7), 1185–1188 (1978).
232. C. Hamel, "Retinitis pigmentosa," *Orphanet. J. Rare Dis.* **1**, 40 (2006).
233. E. L. Berson, "Retinitis pigmentosa: the Friedenwald lecture," *Invest. Ophthalmol. Visual Sci.* **34**(5), 1659–1676 (1993).
234. T. Murakami et al., "Association between abnormal autofluorescence and photoreceptor disorganization in retinitis pigmentosa," *Am. J. Ophthalmol.* **145**(4), 687–694 (2008).
235. C. Dysli et al., "Fundus autofluorescence lifetime patterns in retinitis pigmentosa," *Invest. Ophthalmol. Visual Sci.* **59**(5), 1769–1778 (2018).
236. K. M. Andersen et al., "Characterization of retinitis pigmentosa using fluorescence lifetime imaging ophthalmoscopy (FLIO)," *Transl Vis Sci Technol.* **7**(3), 20 (2018).
237. L. H. Lima et al., "Structural assessment of hyperautofluorescent ring in patients with retinitis pigmentosa," *Retina* **29**(7), 1025–1031 (2009).
238. S. Aizawa et al., "Changes of fundus autofluorescence, photoreceptor inner and outer segment junction line, and visual function in patients with retinitis pigmentosa." *Clin. Exp. Ophthalmol.* **38**(6), 597–604 (2010).
239. S. Kwon et al., "Fluorescence lifetime imaging ophthalmoscopy in early Alzheimer's disease," in *ARVO Annual Meeting*, Honolulu, Hawaii (2018).
240. C. Dysli et al., "Fluorescence lifetime imaging of the ocular fundus in mice," *Invest. Ophthalmol. Visual Sci.* **55**(11), 7206–7215 (2014).
241. C. Dysli et al., "Effect of pharmacologically induced retinal degeneration on retinal autofluorescence lifetimes in mice," *Exp. Eye Res.* **153**, 178–185 (2016).

242. J. Balmer et al., "Retinal cell death caused by sodium iodate involves multiple caspase-dependent and caspase-independent cell-death pathways," *Int. J. Mol. Sci.* **16**(7), 15086–15103 (2015).
243. M. H. Reisenhofer, J. M. Balmer, and V. Enzmann, "What can pharmacological models of retinal degeneration tell us?" *Curr. Mol. Med.* **17**(2), 100–107 (2017).
244. M. Reisenhofer et al., "Multiple programmed cell death pathways are involved in N-methyl-N-nitrosourea-induced photoreceptor degeneration," *Graefe's Arch. Clin. Exp. Ophthalmol.* **253**(5), 721–731 (2015).
245. M. Klemm et al., "Combination of confocal principle and aperture stop separation improves suppression of crystalline lens fluorescence in an eye model," *Biomed. Opt. Express* **7**(9), 3198–3210 (2016).
246. L. Zhang et al., "Volumetric fluorescence retinal imaging in vivo over a 30-degree field of view by oblique scanning laser ophthalmoscopy (oSLO)," *Biomed. Opt. Express* **9**(1), 25–40 (2018).
247. M. A. Digman et al., "The phasor approach to fluorescence lifetime imaging analysis," *Biophys. J.* **94**(2), L14–L16 (2008).

Lydia Sauer received her medical degree from the Friedrich–Schiller-University in Jena, Germany. Currently, she is working as a postdoctoral research associate at the Moran Eye Center of the University of Utah. Her research is focused on functional imaging of the human eyes *in vivo* with a special focus on fluorescence lifetime imaging ophthalmoscopy (FLIO). Her interests include a variety of retinal diseases, such as macular telangiectasia type 2 and age-related macular degeneration.

Karl M. Andersen is a third-year medical student at the Geisinger Commonwealth School of Medicine in Scranton, Pennsylvania. He is originally from Utah where he attended Brigham Young University. As an aspiring ophthalmologist, his research interests include inherited retinal disease and retinal imaging. He is passionate about humanitarian service work, mentoring youth and promoting humanism in medicine.

Chantal Dysli completed an MD–PhD at the Department of Ophthalmology, University Hospital, Bern, Switzerland, after her doctor of medicine. She was working on FLIO in healthy and diseased retina as well as in experimental setups *in vitro* and *in vivo*. Currently, she is completing her residency in ophthalmology in Bern and Bonn. Her special field of interest and research is multimodal retinal imaging including fluorescence lifetime imaging ophthalmoscopy.

Martin S. Zinkernagel is a consultant ophthalmic surgeon at the Department of Ophthalmology, University Hospital of Bern, Switzerland. He earned his MD from the University of Zurich and PhD for his studies in ocular immunology at the University of Western Australia. His clinical research interests are multimodal retinal imaging, microbiome research, artificial intelligence in retinal imaging, and innovative surgical techniques. Basic research interests include ocular immunology, *in vivo* imaging and the role of the innate immune system in retinal degeneration.

Paul S. Bernstein joined the faculty of the Moran Eye Center of the University of Utah in 1995, where he currently divides his time equally between clinical and basic science retina research and a clinical practice devoted to medical and surgical treatment of disease of the retina and vitreous with special emphasis on macular and retinal degenerations. His current research interests are focused on the biochemistry and biophysics of nutritional interventions against inherited and acquired ocular disorders.

Martin Hammer received his PhD in physics in 1999 from the University of Jena. From 1983 to 1990, he worked at the R&D Department of Carl Zeiss Jena. Since 1990, he is with the University Hospital Jena. He is the head of the experimental ophthalmology group. His current research interest is functional and molecular imaging at the retina. He works on retinal oximetry and blood flow and on the investigation of intrinsic fluorophores at ocular fundus.